LSU Master's Theses   Graduate School

2012

Linear PM generator for wave energy conversion

Rajkumar Parthasarathy
Louisiana State University and Agricultural and Mechanical College, sarathyraj16@gmail.com

LINEAR PM GENERATOR FOR WAVE ENERGY CONVERSION

A Thesis

Submitted to the Graduate Faculty of the
Louisiana State University and
Agricultural and Mechanical College
in partial fulfillment of the
requirements for the degree of
Master of Science in Electrical Engineering

in
The Department of Electrical and Computer Engineering

by
Rajkumar Parthasarathy
Bachelor of Engineering, Anna University, 2008
May 2012

DEDICATION

To my parents,

ACKNOWLEDGEMENTS

TABLE OF CONTENTS

LIST OF TABLES

LIST OF FIGURES

viii

ABSTRACT

The main objective of this thesis is to design a selected version of linear PM generator and to determine the electromechanical characteristics at variable operating conditions. To reach this objective, the linear generator with quasi-flat linear machine structure was selected and designed using the magnetic circuit theory. By applying 2-D and 3-D FEM the magnetic circuit was optimized and parameters of equivalent circuit were determined.

The performance of generator operation are analyzed in steady-state and in dynamic conditions using MATLAB/SIMULINK. The analysis has been carried out at the secondary variable speed, which is changing sinusoidally according to the motion of the sea waves. The output and the input powers of the generator at rated speed of 2.2 m/s are 34KW and 40KW respectively. The maximun output power is generated when the generator is connected to a resistive load of 7.5Ω. The efficiency obtained for rated average speed of 1.4 m/s and at rated load resistance (of 7.5Ω) is equal to 85%.

CHAPTER 1

INTRODUCTION

Linear generators are used nowadays in the field of sea wave energy conversion (WEC). Since wave energy is available in adequate and it is considered to be renewable, a lot of research is conducted in the field of WEC [1]. Paper [2] discusses the various other types used in WEC techniques, Turbine type and Buoy type are some of the prominent types used in the WEC. Archimedes Wave Swing (AWS) is also one of WEC system.

1.1 Literature Review on Archimedes Wave Swing System

"Archimedes Wave Swing (AWS) is one, which converts the wave energy of the ocean to electrical energy" [3]. Of all the WEC types, AWS is considered more advantageous. AWS is normally submerged totally inside the sea according to paper [3] making it more convenient for the ships to move without any hurdle. It is also considered to take less space producing high power density according to paper [2].
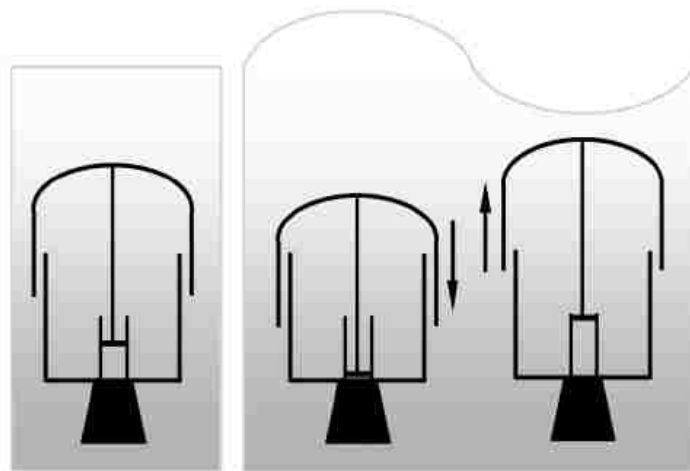
Figure 1.1 Configuration of AWS [4]

The figure1.1 gives the basic concept of AWS system. It consists of two parts. One is a moveable top floating part and the other part is fixed to the bottom of the sea (see figure 1.1). The AWS is an air filled chamber, which is cylindrical in shape. When there is a wave, the amount of pressure due to more water causes the top floater part to move downwards. When the wave moves away there is less pressure and the air filled in the chamber tends to push the top part to its position acting as a spring. This linear motion generator is the main idea behind generating electricity. This AWS concept was used in few papers [3, 5, 6] in the design of linear generator for marine application. According to paper [7], Professor Dr. Polinder had made a great contribution in solving many problems related to the linear generators which is presented in paper [3]. Hence, his paper on modeling the wave power device was instrumental throughout the thesis work.

AWS system uses PM linear generator for the generation of electrical energy. Few types of the PM linear generator are,

- Tubular PM linear generator
- Flat PM linear generator

1.1.1 Tubular Type PM Linear Generator

Generator shown in figure 1.2 is one of the few types of tubular PM linear generators. As the name suggest the shape of the generator is cylindrical. The principle of operation is the same as that of the AWS. The translator (slider) acts as the rotor that moves linearly while the stator is fixed. Permanent Magnets are attached to the slider whereas the stator carries the windings. Due to the wave motion the translator is moving up and down linearly. Since the
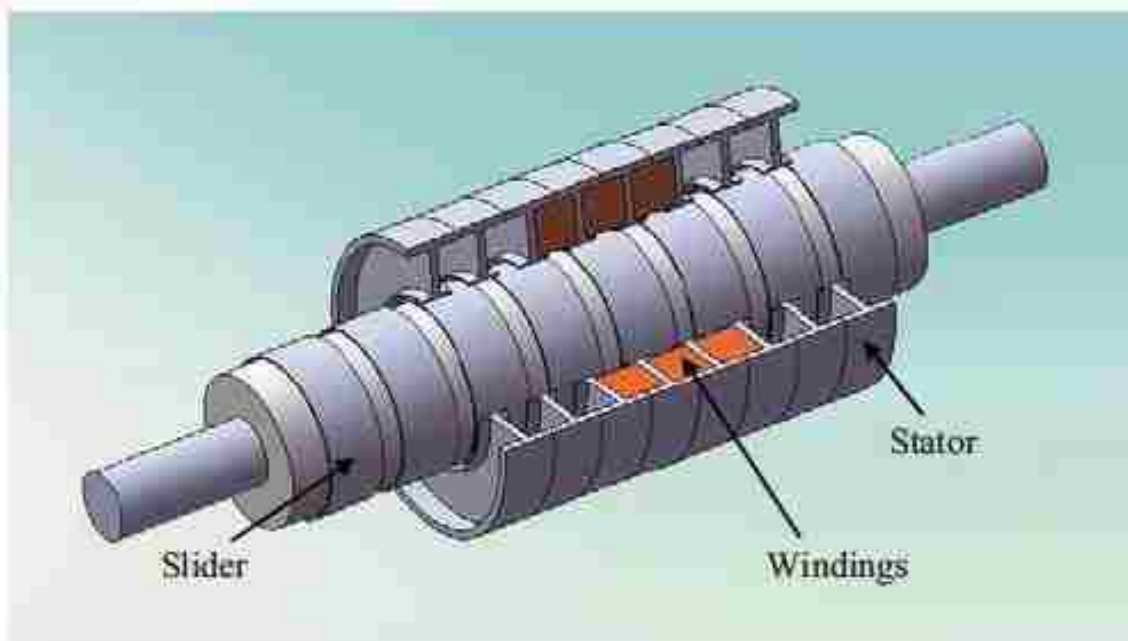
Figure 1.2 Tubular PM linear generator [8]

translator has magnet on it, it produces strong magnetic field, which cuts the winding, inducing electricity described by Maxwell theory. In the papers [7, 8] the authors describes a individual approach for the design of the generator and then designed using FEM (Finite Element Method). Paper [9] talks about the advantages of using a tubular design and also explains the wave energy conversion associated with this design.

1.1.2 Flat Type PM Linear Generator

This is a flat type double-sided PM linear generator. The principle of operation is the same as that of the tubular type generator. Even though many papers present tubular generator design for AWS but still a "flat type is cheap and very easy to build" [11]. The paper [10] talks about the advantages of a flat type over the cylindrical type. It also says that the efficiency, output power, current and voltage has increased by the use of the flat type structure. It can be used for AWS concept for the generation of electricity from wave energy. This paper

3
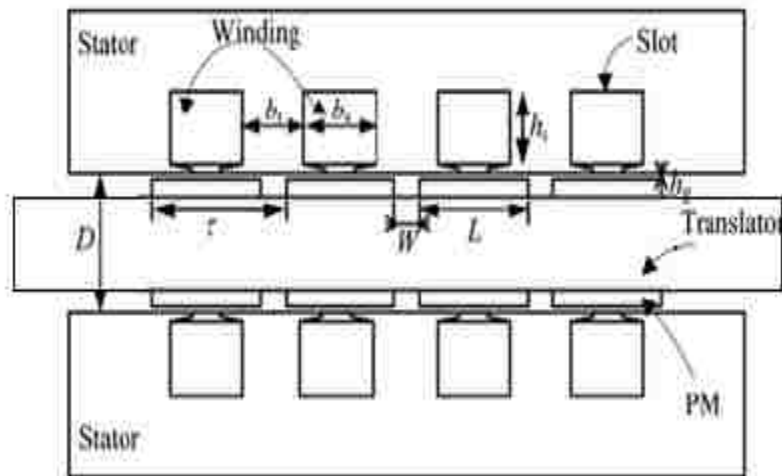
Figure 1.3 Flat type PM linear generator [10]

suggests that by changing the dimensions we can get optimal design. This will be very useful in the optimizing of the generator, which will be discussed later on chapter 4.

The objective of this thesis is to use some of the results shown in papers [3, 7, 10] to design an efficient quasi-flat linear PM generator for wave energy conversion. After the designing is done, a dynamic analysis is carried out in different operating conditions.

1.2 Objective of Thesis

- To design and optimize a quasi-flat tubular linear PM generator.
- To determine the generator electromechanical characteristics in variable operating conditions.

1.3 Task to Be Done

- To determine the winding parameters and dimensions of the rotor and stator using analytical approach.
- To build the 2-D model for optimization of stator and rotor cores.

- To build a 3-D motor model in FEM using Ansoft Maxwell v12 software:
    - ➢ To determine the flux density distribution,
    - ➢ To find electromechanical parameters of generator.
- To find terminal voltage at average speed using equivalent synchronous generator circuit.
- To build Simulink generator model and to analyze its performance in dynamic conditions.

1.4 Outline of Thesis

Chapter 2 presents the steps used in Ansoft Maxwell V12 for the design of the generator.

Chapter 3 explains the general structure, and the design parameter in detail.

Chapter 4 discusses the optimization of the generator model in 2-D FEM and the electromechanical parameters are found from 3-D model.

In chapter 5 MATLAB SIMULINK model is developed and performance of the generator is analyzed at variable secondary speed.

Finally, in chapter 6 the conclusion and future scope of study is written.

CHAPTER 2

PERMANENT MAGNET GENERATOR MODELING IN FEM

Once the winding parameters and core dimensions are found, modeling and finding the electromechanical parameters of the generator plays a major role. For this, Maxwell Ansoft v12 software is used to solve all magnetostatic problems. These problems are described by the Maxwell differential equations.

2.1 Maxwell Equation

Maxwell equations embrace the equations that were earlier derived for electric and magnetic phenomena. One of them is,

Ampere's law:

$$\nabla \times H = J \tag{2.1}$$

where, J - current density

H - field intensity

From Gauss law:

$$\nabla \cdot B = 0 \tag{2.2}$$

magnetic flux density B can be related to H as:

$$B = \mu \cdot H \tag{2.3}$$

If it is a nonlinear material, the permeability is a function of B:

$$\mu = \frac{B}{H(B)} \tag{2.4}$$

Flux density B can be expressed in terms of vector potential A as:

$$B = \nabla \times A \tag{2.5}$$

Hence, from equation 2.1 and 2.2:

$$\nabla \times \left(\frac{1}{\mu(B)} \nabla \times A \right) \tag{2.6}$$

6

FEM is a numerical method that allows solving equation (2.6) used for magnetostatic problems with nonlinear B-H relationships.

2.2 Modeling by MAXWELL 12v Program [12]

"Maxwell is a computer operated interactive software that uses finite element analysis to solve 3D (3-dimensional) magneto static problem. For the purpose of designing and analyzing of electric machines model, Rotational Machine Expert (RMxprt) software is used" [12].

2.2.1 Maxwell Desktop
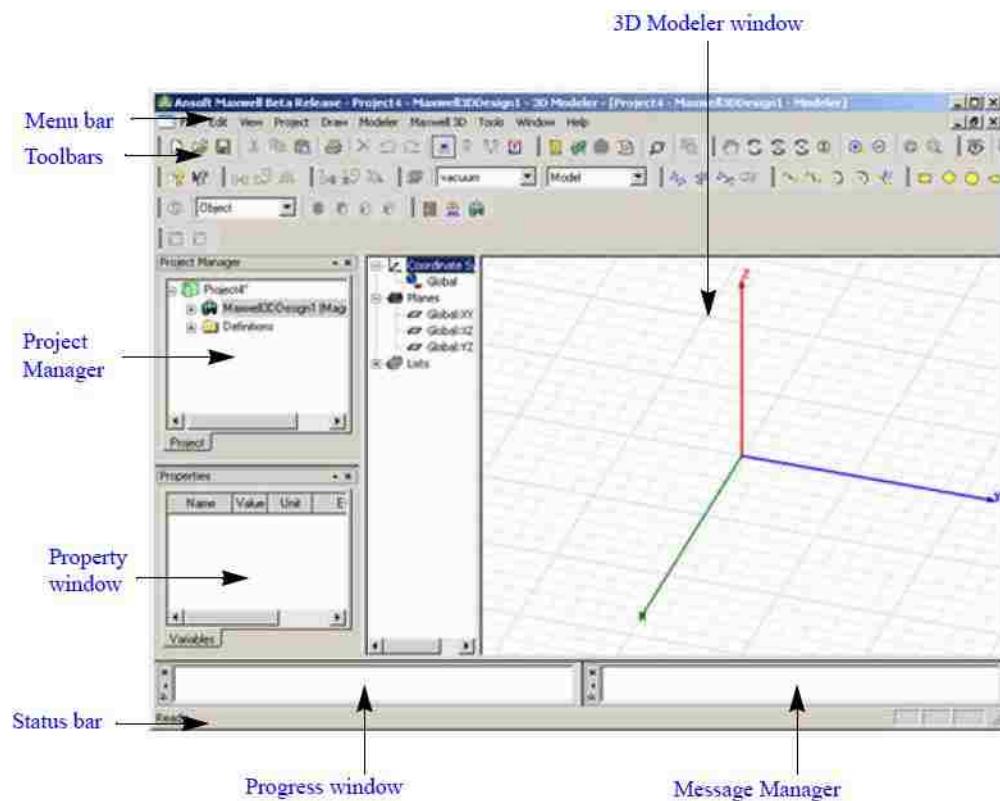
Figure 2.1 Maxwell desktop window [12]

The figure 2.1 is the screenshot of the Maxwell v12 desktop. It appears when we launch the software. The parts of the windows, which are clearly marked, are used in the designing the model.

7

- **Menu bar**- The menu bar is used for working with various Maxwell tasks, which include creating new project, opening new project, editing, drawing, help with the software etc.

- **Tool bar** – Tool bar has a list of shortcut icons, which are available in the menu bar. Most of the frequently used commands like new windows, save, etc. items are default present. We can also customize this bar by including or removing tools from this bar.

- **Project Manager** – Project manager has the project structure of the project that is running on the Maxwell. It is structured like a tree with the project title as the main followed by the boundaries, excitations, analysis and results.

- **Property window** – It is a window (see figure 2.2) where we can see the properties or values of the items that are clicked in the project tree or in the Maxwell 3D modeler window. We can assign or edit values in this window of any particular selected items.
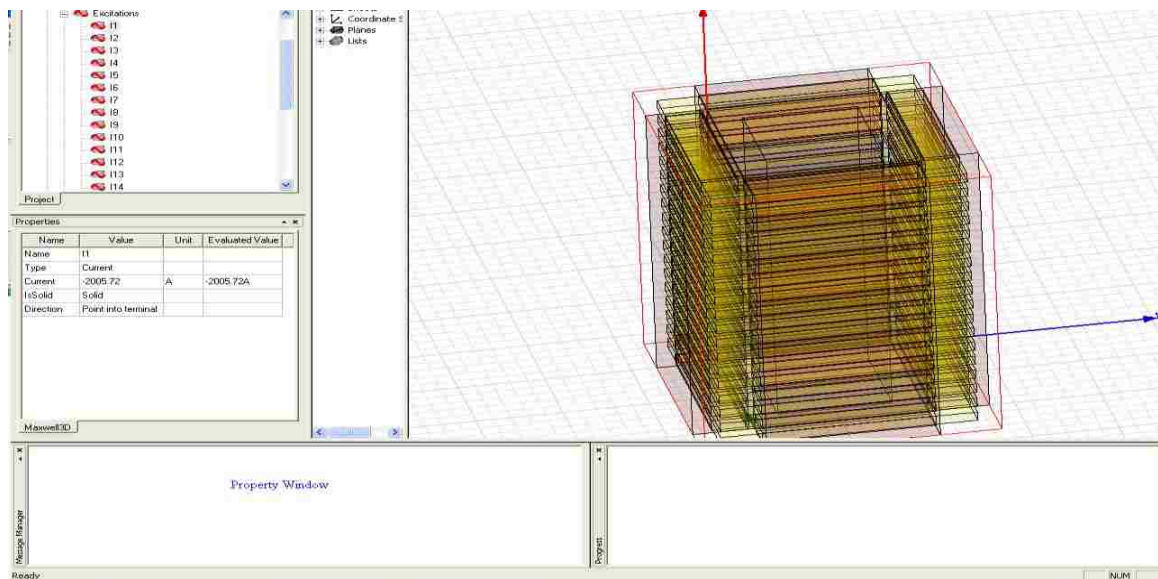
Figure 2.2 Property windows

- **3D Modeler window** – Modeler window can also be called as the model workspace. It is the window where the model is created. Since it's a 3D model, this window has a default direction marker with X, Y and Z directions with grids.

2.2.2 Drawing Tool

Maxwell v12 allows us to draw 1D, 2D and 3D electromagnetic model. Drawing tool are a collection of tools used to draw the model in the modeler window. First step is to open the new project for drawing the model. For this, user can select File from the main menu and then click new project. The new project file with a default name "project1" will be displayed on the project manager window. Then double click on the project file in the project tree to open it. There are many drawing tool features available in the main menu.

- **One-dimensional 1D**– 1D objects include the straight line or arc line or spline segments. User can access them by clicking the following icon . All these together are called as polylines. As the name suggest it doesn't have any volume or surface associated with it. It has a start point and end point.

- **Two-dimensional 2D** – 2D objects include rectangle, arc or circles, etc. These two dimensional figures are closed sheet objects. Clicking the following icon can access them . They are always enclosed within a boundary.
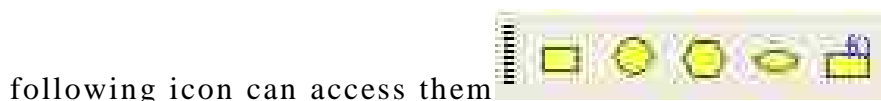
- **Three-dimensional 3D** – 3D objects include objects like cylinder, boxes, cones and spheres. A 2D object can be manipulated to a 3D object by

9

using the DRAW command. User can access them by clinking the following icon .

In order to draw a box, user has to select "draw" from the menu bar and then select "box" or we can directly select it from the shortcut available. In order to give the corner base, we can either click the point in the grid using a mouse or we can give the starting points i.e. X, Y and Z co-ordinates in the message box. The other point in relative to the previous point can be specified in dX, dY and dZ.

Other features of the design include cutting, splitting, separating and combining parts. This feature can be used with the Boolean function in the modeler menu. An example of a Boolean function is shown in figure 2.3. There are many other editing tool bars available like the mirroring objects, offsetting objects, duplicating objects etc.
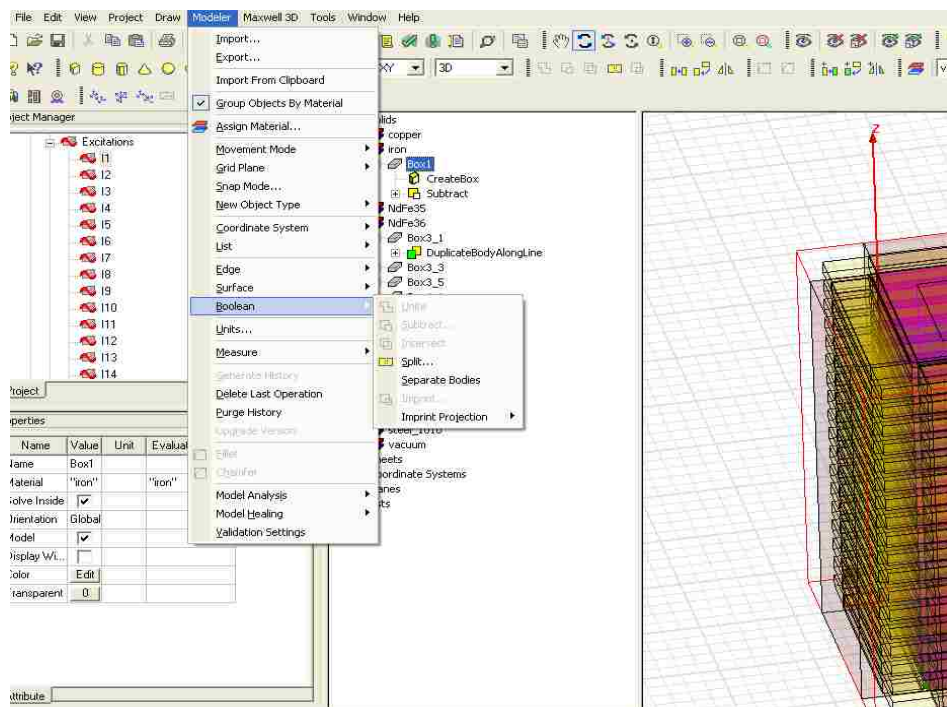
Figure 2.3 Example for a Boolean function

10

2.2.3 Preprocessor Mode

The most important part of the designing task is assigning of materials to each part of the model. It is very important for the user to assign material properties because it gives an actual result, which will be obtained practically. There are many materials available in this software. User can assign materials by clicking the following icon [icon]. The other way is to first select the part, to which the material has to be added and click Modeler -> Assign material. A Select definition dialog box appears as show in the figure 2.4. By default the Ansoft's entire material library and the local project's material library are displayed in it. Maxwell 12v allows setup of magneto static, electrostatic, DC conduction and 3D transient boundary condition. User has to assign the exact
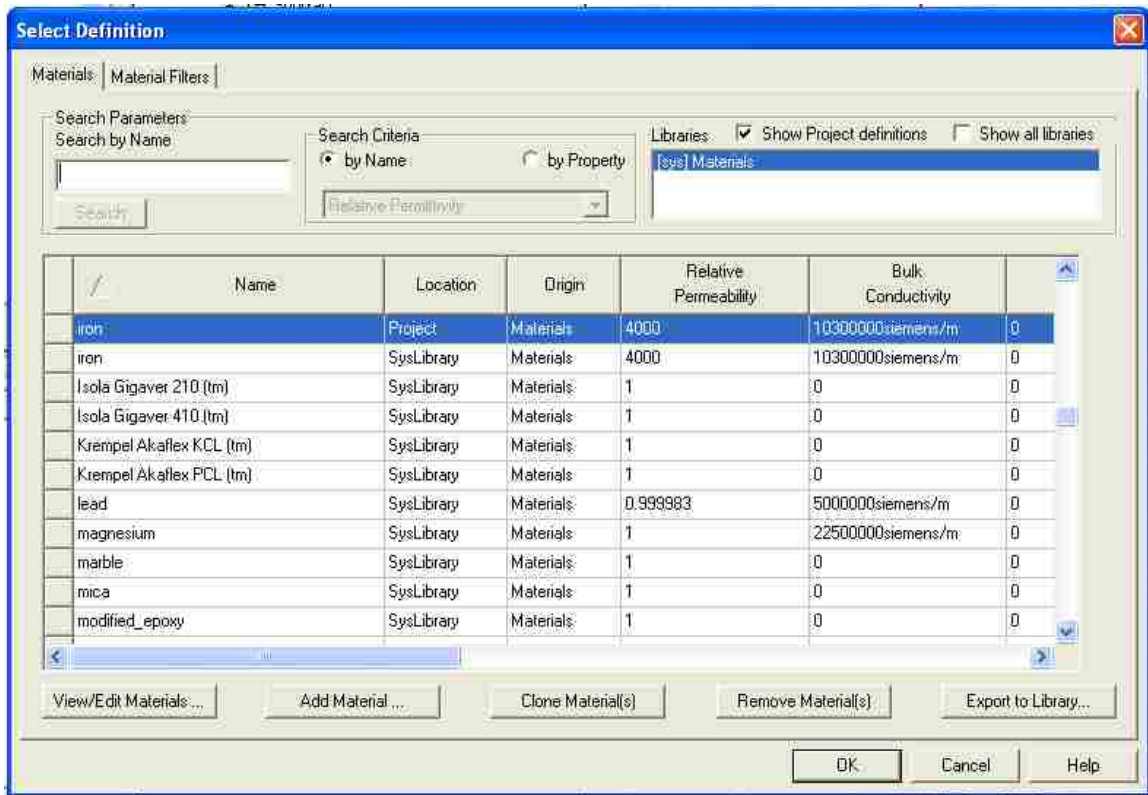
Figure 2.4 Select Definition windows for assigning materials

value of voltage, current, number of winding, or current flow direction. The direction of flow of current element determines the operation of the system so the user must take care to assign them properly.

2.2.4 Postprocessor Mode

This is the final step of getting results from the model designed. Problems such as the force, torque and self-inductance can be solved using the Maxwell 12v. User can assign force or torque parameters by selecting the object, part for which the parameter has to be found. It can be done by selecting parameters (Fig 2.5).

"Passes" are normally given to check the solution accuracy. Normally the user can use 3 to 10 passes depending on the complexity of the model. Apart from the passes the error percent is also mentioned, which can be set as 0.01 percent.
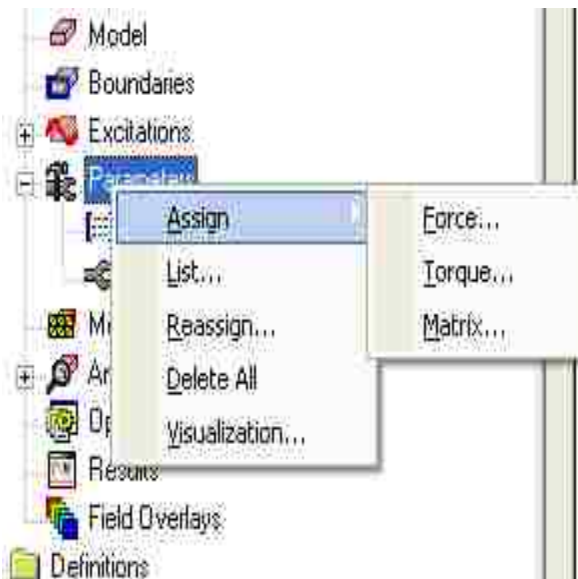
Figure 2.5 Assigning of Force and torque

Then the type of force that has to be found and also an axis direction that has to be assigned. Next comes the function of Matrix setting, by selecting parameters-> assign-> matrix. Once the simulation is over the user can get the values of inductance of each of the coil by clicking the matrix button.

The last step before simulating is to check whether the model is correctly designed. By clicking the software tells the user if there is any error in any part of the model. This step is done till the model has no errors.

Once the Validation check is over the model is analyzed to find the solutions. Once the simulation is over the message is prompted in the progressing windows, which say that the simulation is successfully completed. The results can be obtained by clicking which generates the report and is used to plot magnetic flux, magnetic flux density and current density distribution.

CHAPTER 3

QUASI-FLAT TUBULAR LINEAR PM GENERATOR

3.1 General Description

The proposed structure of PM linear generator is shown schematically in figure 3.1. It consists of four flat primary parts and four secondary parts
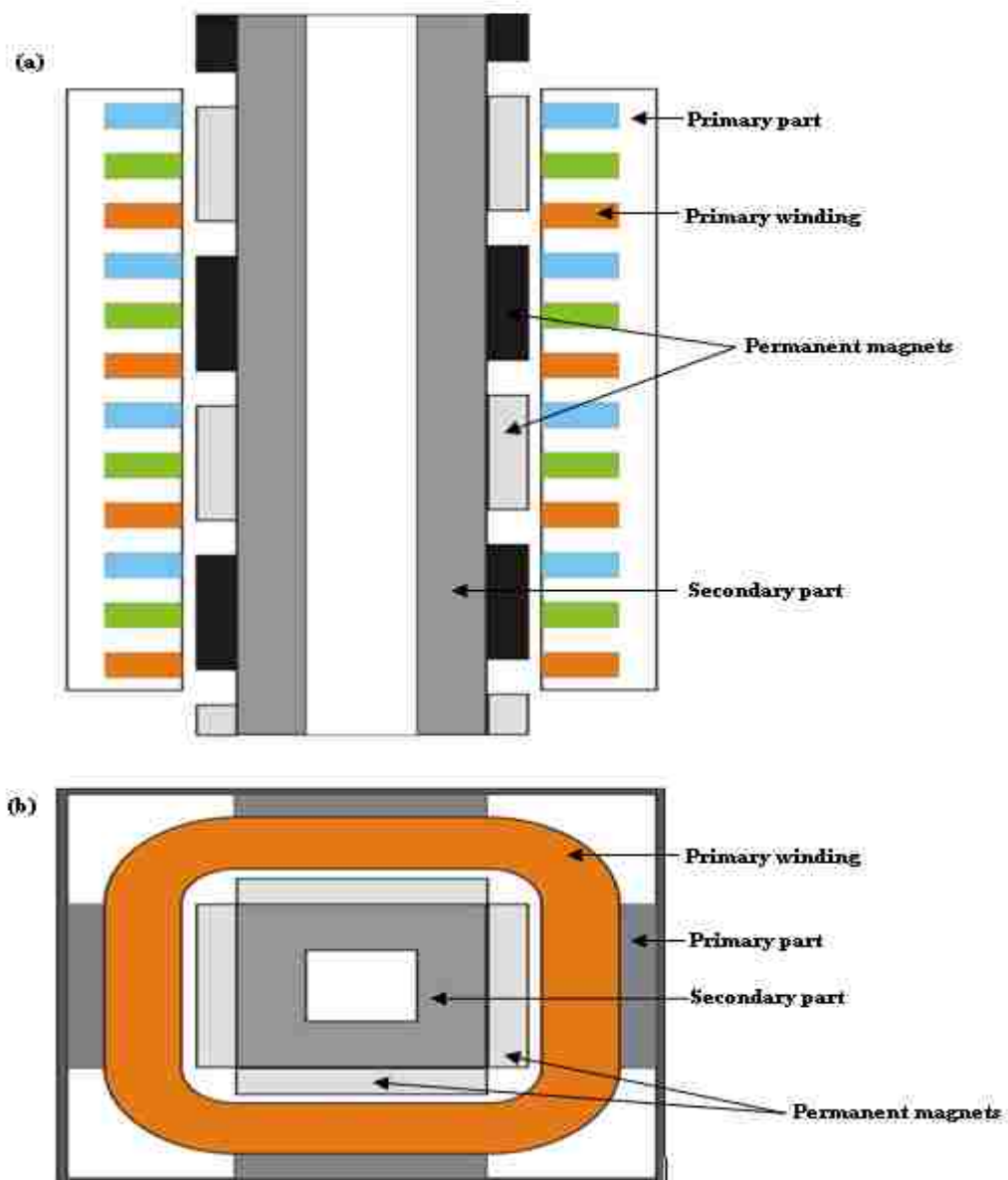
Figure 3.1 General Model of Quasi-Flat tubular PM generator:
- longitudinal cross-section (b) – top-view

enclosed within one housing. Each of the flat parts reminds of a flat linear machine as shown in figure 3.2.
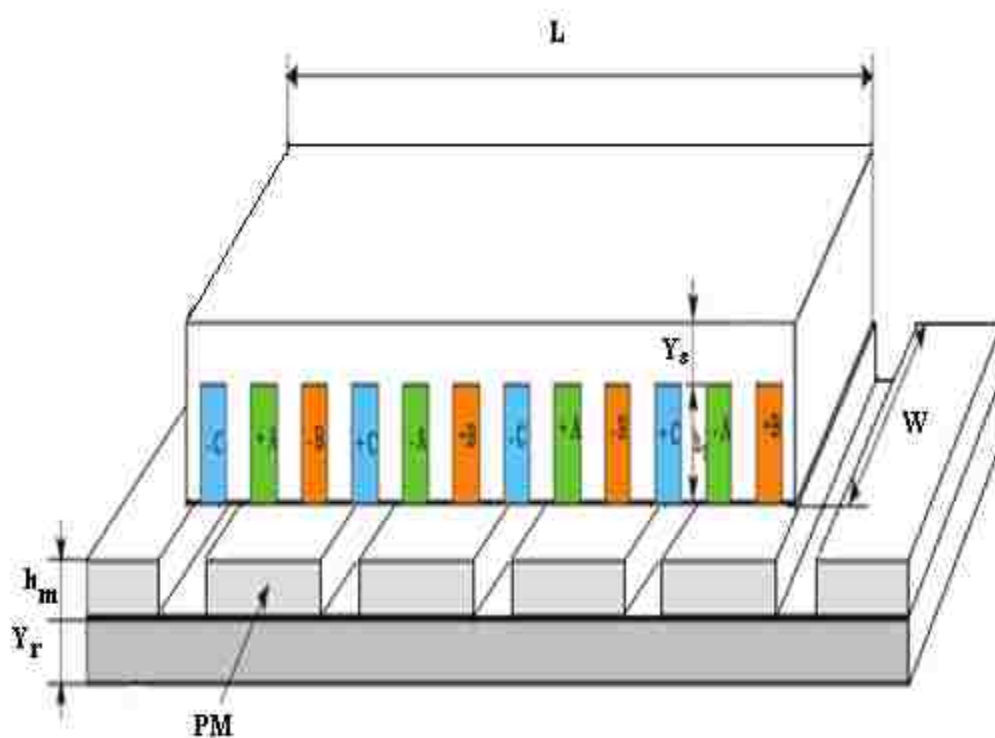
Figure 3.2 Structure of flat linear PM generator

In this design version, the primary part is shorter than the secondary part. Furthermore, the primary has 3-phase winding placed in the slots. A secondary part consists of ferromagnetic plate and PM's glued to its surface. Another solution is the secondary part with buried PM's as shown in figure 3.3. The PM linear generator considered in this thesis (see figure 3.1) has similar structure as flat linear machine but its winding remains the 3-phase winding of tubular motor shown in figure 3.4. In this solution the winding consists of coaxial coils surrounding the secondary part.

(a)   (b)
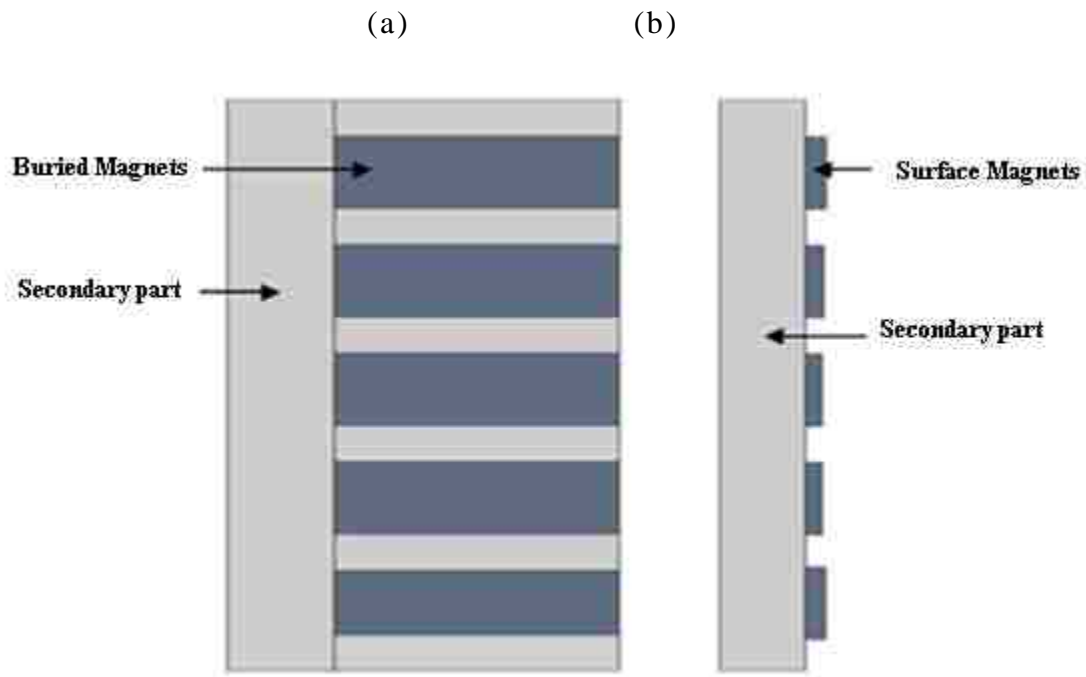
Figure 3.3 Secondary part structure with (a) buried type magnets and (b) surface mounted magnets
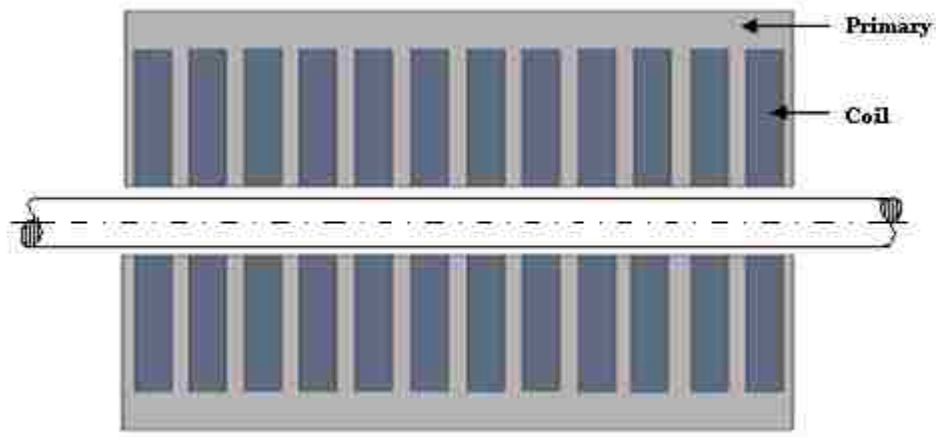
Figure 3.4 Three-phase winding of tubular motor

In the proposed structure (figure 3.1) the four flat primary cores have common 3-phase winding. This justifies the name of this generator, which is called quasi flat tubular PM linear generator. The short primary part is stationary, while the secondary moving part with the PM's being attached to the

16

floater (see figure 1.1). This relative motion between two generator parts causes the electromotive force (e) to be induced in the winding according to the general equation:

$$e = \frac{d\lambda}{dt}$$ (3.1)

where,

λ = is the flux linkage of the particular winding

3.2 Determination of Generator Core and Winding Parameters

3.2.1 Assumptions of Generator Model

The generator model that will be used in design calculations is described by the following assumptions:

- The magnetic permeability of the primary and the secondary cores are infinitely high (μ_{c1}, $\mu_{c2} = \infty$)

- Floater velocity v_{rm} is changing sinusoidally in time.

- Flux density B in the air-gap is changing sinusoidally in the direction of the motion according to the equation:

$$B(z) = B_m \cos(\frac{\pi}{\tau}z)$$ (3.2)

where, τ = pole pitch

- Flux linkage λ of each phase changes sinusoidally in time and for phase A:

$$\lambda_A = \lambda_m \sin\omega t$$ (3.3)

- The primary part is replaced by the unslotted core with the infinitely thin current layer as shown in figure 3.5.

17

Figure 3.5 Schematic representation of unslotted primary core

The real air-gap is replaced by the equivalent one calculated as:

$$g_{eq} = K_c \; g \qquad\qquad (3.4)$$

where K_c is the Carter's coefficient and is calculated from the equation [9]:

$$K_c = \frac{\tau_t \, (s_E + b_s)}{(\tau_t \, (s_E + b_s) - b_s)^2} \qquad\qquad (3.5)$$

This coefficient includes the increase of air-gap caused by stator slotting.

3.2.2 Designing Calculation

The initial data of the generator to be designed are as follows:

➢ Input apparent power S_{in} = 36KVA;

➢ Induced phase voltage $E = 600/\sqrt{3} = 346.4$ V;

➢ Floater velocity amplitude v_{rm} (changing sinusoidally) = 2.2 m/s;

➢ Average floater velocity $v_{av} = \frac{2}{\pi} v_{rm}$ = 1.4006 m/s

➢ Number of phases m = 3;

➢ Number of slots/pole/phase q =1;

18

- ➤ Number of poles p = 6;

- ➤ Average flux density in air gap B_g = 0.8 T;

- ➤ Coefficient for air-gap flux density $C_m = B_g/B_m$ = 0.9,

  where B_m = air-gap flux density under magnets;

- ➤ Air gap g = 0.002 m;

- ➤ Permissible flux density in stator core B_y^s = 1.8 T;

- ➤ Permissible flux density in rotor core B_y^r = 1.2 T;

- ➤ Current loading (linear current density of the stator) J = 120 KA/m;

- ➤ Wire current density J_w = 5 A/mm^2;

- ➤ Winding filling factor K_{cu} = 0.6;

❖ **Primary length and width**

The input power S_{in} when ignoring the mechanical losses is given by the equation:

$$S_{in} = m \ E_{ph} \ I_{ph} \qquad (3.6)$$

where: E_{ph} – Phase induced voltage

I_{ph} – Phase current

When the magnets are moving with speed v_{av} with respect to the phase coils the electromotive force is induced and its maximum value (see figure 3.6) at maximum flux density B_m ($B(z) = B_m \cos(\frac{\pi}{\tau}z)$) what was assumed) is:

$$E_{ph \ m} = M_s \cdot W_s \cdot N_{ph} \cdot B_m \cdot v_{av} \qquad (3.7)$$

Thus the rms emf:

$$E_{ph} = \frac{M_s \cdot W_s \cdot N_{ph} \cdot B_m \cdot v_{av}}{\sqrt{2}} \tag{3.8}$$
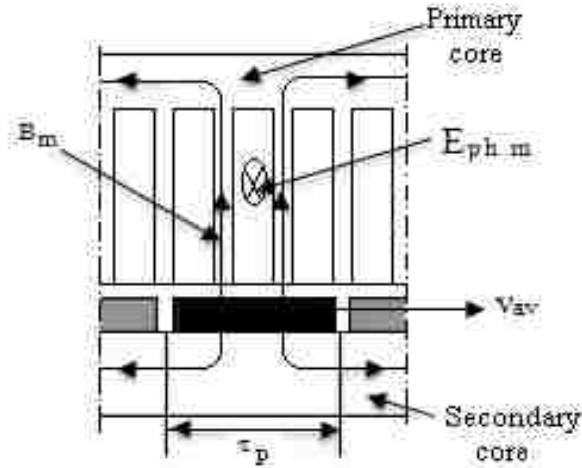
Figure 3.6 Generator model of Eqn. 3.7

The phase current can be expressed in terms of current loading J which is described by the equation:

$$J = \frac{N_s I_{ph}}{\tau_t} \tag{3.9}$$

where: N_s – number of turns per coil

$\quad \tau_t$ – tooth pitch

Thus the phase current:

$$I_{ph} = \frac{J \tau_t}{N_s} \tag{3.10}$$

The number of wire per slot N_s can be expressed in terms of number of turns per phase N_{ph} calculated as:

$$N_{ph} = N_s \cdot q \cdot p \tag{3.11}$$

$$N_s = \frac{N_{ph}}{q \cdot p} \tag{3.12}$$

20
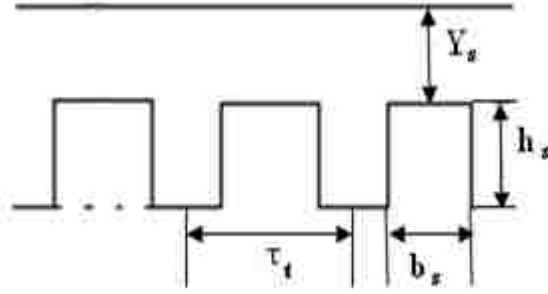
Figure 3.7 Picture showing primary core slots

Substituting Eqns. 3.8, 3.10 and 3.12 in to Eqn. 3.6, we obtain:

$$S_{in} = m \, \frac{M_s \cdot W_s \cdot \tau_t \cdot p \cdot q \cdot m \cdot B_m \cdot v_{av} \cdot J}{\sqrt{2}} \tag{3.13}$$

Since the stator length is:

$$L_s = \tau_t \cdot p \cdot q \cdot m \tag{3.14}$$

The input power is:

$$S_{in} = \frac{m}{\sqrt{2}} \cdot M_s \cdot W_s \cdot L_s \cdot B_m \cdot v_{av} \cdot J \tag{3.15}$$

In calculation it is assumed that $W_s = 0.2m$. Thus, the length of the stator is:

$$L_s = \frac{S_{in} \sqrt{2}}{M_s B_m J v_{av} W_s} \tag{3.16}$$

$$L_s = \frac{36000 \cdot \sqrt{2}}{4 \cdot 0.88 \cdot 120000 \cdot 200 \cdot 1.40006} = 432 \text{ mm}$$

❖ **Pole pitch and tooth pitch:**

The pole pitch τ_p is:

$$\tau_p = \frac{L_s}{p} \tag{3.17}$$

21

$$\tau_p = \frac{432}{6} = 72 \text{ mm}$$

The tooth pitch τ_t can be found from :

$$\tau_t = \frac{\tau}{(m \cdot q)} \tag{3.18}$$

$$\tau_t = \frac{72}{(3 \cdot 1)} = 24 \text{ mm}$$

❖ Slot and tooth dimensions

Slot width b_s can be calculated from τ_t as shown in figure 3.7:

$$\tau_t = b_S + b_t \tag{3.19}$$

Assuming $b_t = \frac{1}{2} \, b_S$, the slot opening is:

$$b_s = \frac{2}{3} \, \tau_t \tag{3.20}$$

$$b_s = \frac{2}{3} \cdot 24 = 16 \text{ mm}$$

and tooth width:

$$b_t = 1/3 \, \tau_t \tag{3.21}$$

$$b_t = \frac{1}{3} \cdot 24 = 8 \text{ mm}$$

❖ Permanent magnet dimensions

From Eqn. 3.5, Carter's coefficient K_c has to be found in order to calculate the equivalent air-gap g_{eq}:

$$K_C = \frac{\tau_t \, (s_g + b_s)}{(\tau_t \, (s_g + b_s) - b_s^2} \tag{3.22}$$

$$K_C = \frac{(0.024 \; (5 \cdot 0.002 + 0.004))}{(0.02 \; (5 \cdot 0.002 + 0.004) - (0.004 \cdot 0.004))}$$

$$K_C = 1.05$$

now,

$$g_{eq} = K_C \cdot g \tag{3.23}$$

$$g_{eq} = 1.05 \cdot 0.002 = 0.0021 \text{ m}$$

To determine the thickness of the magnet, it is assumed that the primary and the secondary permeability $\mu_c = \infty$. According to Ampere's law:

$$\oint H \, dl = iN \tag{3.24}$$

When applied to the generator magnetic circuit shown in figure 3.8 it takes the form:

$$2 \; H_m \; h_m + 2 \; H_g \; g_{eq} = 0 \tag{3.25}$$

After transformation the field intensity in the air-gap:

$$H_g = (-h_m / g_{eq}) \; H_m \tag{3.26}$$

After multiplying by μ_0, the flux density in the air-gap:

$$B_g = (- h_m / g_{eq}) \; H_m \; \mu_0 \tag{3.27}$$
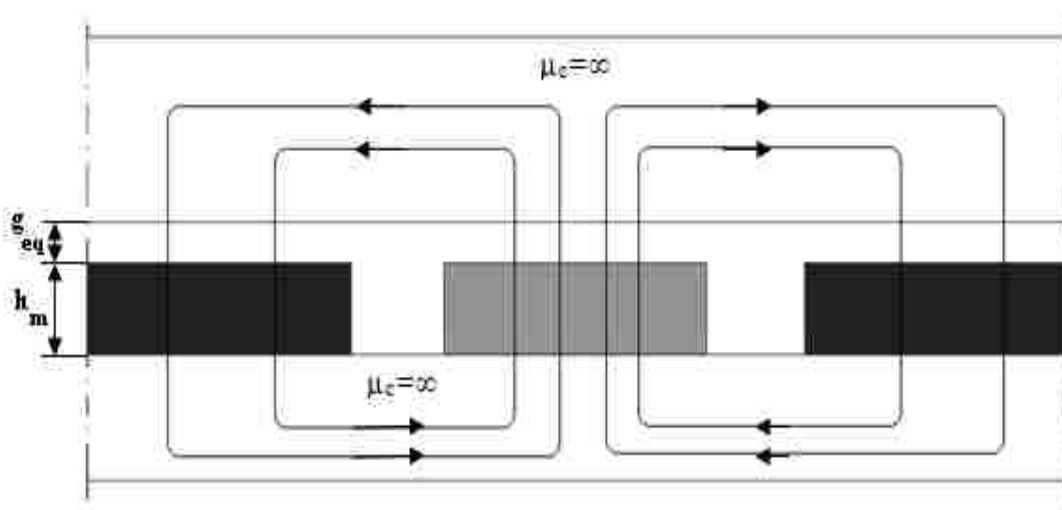
Figure 3.8 Model of generator with unslotted primary core
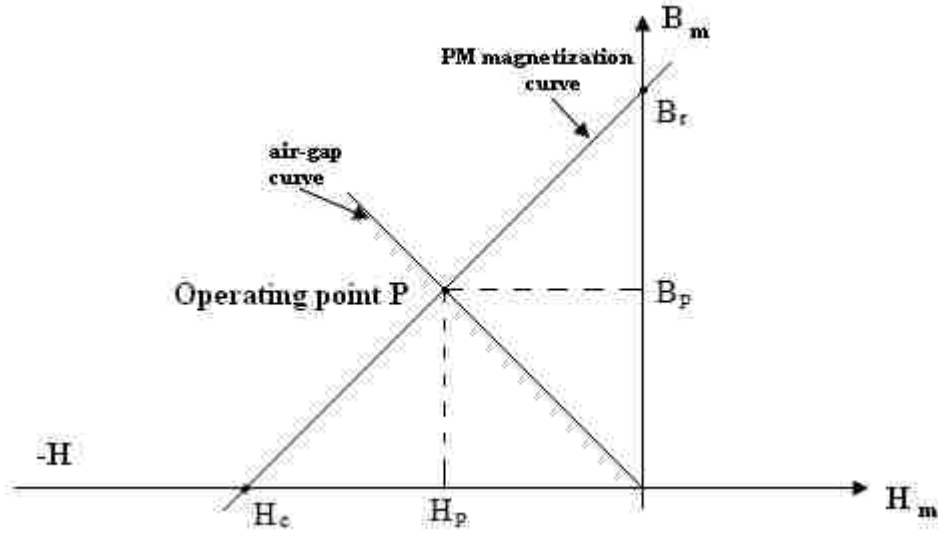
Figure 3.9 Demagnetization B-H curve in air-gap

Since for NdFeB magnets the demagnetization curve is a straight line (figure 3.9) this curve can be described by the equation:

$$B_m = \frac{B_r}{|H_c|} H_m + B_r \tag{3.28}$$

After its modification:

$$H_m = \frac{(B_m - B_r)|H_c|}{B_r} \tag{3.29}$$

Since the flux density in the air-gap is the same as in the permanent magnets $(B_m = B_g)$ hence inserting Eqns. 3.29 and 3.27 we obtain:

$$B_g = \left(\frac{-h_m}{g_{eq}}\right) \frac{B_m - B_r}{B_r} |H_c| \mu_0 \tag{3.30}$$

Thus:

$$h_m = \frac{g_{eq} B_g B_r}{\mu_0 |H_c| (B_r - B_g)} \tag{3.31}$$

where B_g is the average flux density in the air-gap

For $g_{eq} = 0.0021$m, $B_g = 0.8$ T, $B_r = 1.2$ T and $|H_c| = 905000$

24

$$h_m = \frac{2.1 \cdot 0.8 \cdot 1.2}{1.256 \cdot 905000(1.2-0.8)} \qquad (3.32)$$

$$h_m = 6mm$$

Yoke dimensions

Stator yoke thickness Y_S:

Looking at the figure 3.10 the flux in the air-gap is,

$$\Phi_g = \tau \cdot W_s \cdot B_g \qquad (3.33)$$

The flux in the primary yoke:

$$\Phi_y^s = Y_s \cdot W_s \cdot B_y^s \qquad (3.34)$$

Since $\Phi_g = 2\Phi_y^s$, from Eqns. 3.33 and 3.34 we get:

$$Y_S = \frac{B_g}{B_y^s}\frac{\tau}{2} \qquad (3.35)$$

$$Y_S = \frac{0.8}{1.8} \cdot \frac{72}{2} = 16 \text{ mm}$$
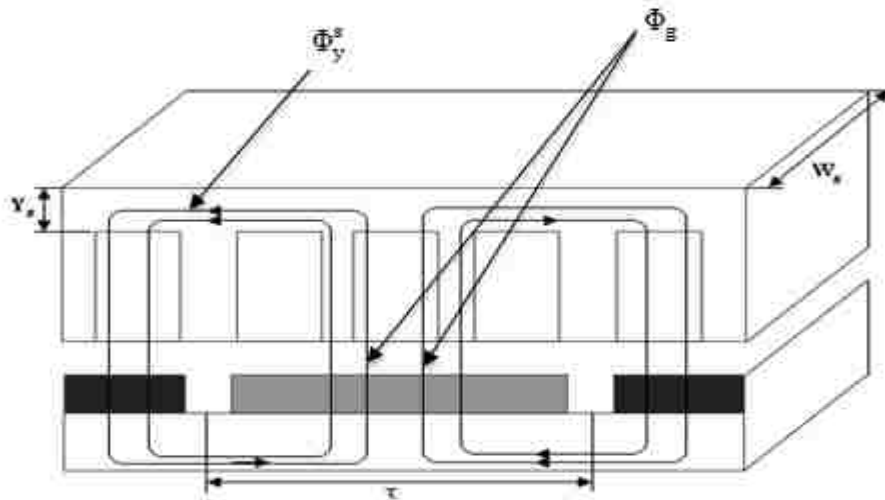
Figure 3.10 Model for finding the yoke dimensions

Rotor yoke thickness Y_r:

The thickness of the secondary yoke can be determined in similar way as done for the primary yoke and thus we have:

$$Y_r = \frac{B_g}{B_y^r} \frac{\tau}{2}$$ (3.36)

$$Y_r = \frac{0.8}{1.2} \cdot \frac{72}{2} = 24 \text{mm}$$

❖ **Permanent Magnet length**

$$\tau_m = C_m \cdot \tau$$ (3.37)

$$\tau_m = 0.9 \times 72 = 64.8 \text{ mm}$$

Generator winding parameters:

❖ Electromotive force E_{ph} (from Eqn. 3.8)

$$E_{ph} = \frac{M_g \cdot W_g \cdot N_{ph} \cdot B_m \cdot v_{av}}{\sqrt{2}}$$ (3.38)

❖ The number of turns per phase N_{ph} can be obtained by re-arranging Eqn. 3.38

$$N_{ph} = \frac{E_{ph} \sqrt{2}}{(M_g \cdot B_m \cdot W_g \cdot v_{av})}$$ (3.39)

$$N_{ph} = \frac{346.48 \sqrt{2}}{(4 \cdot 0.88 \cdot 200 \cdot 1.4 \cdot 10^3)} = 491 \text{turns}$$

❖ Number of turns per coils N_c:

$$N_c = \frac{N_{ph}}{(p \cdot q)}$$ (3.40)

$$N_c = \frac{491}{(6 \cdot 1)} = 82 \text{ turns}$$

❖ For a three phase Y connection the value of rms current I:

$$I = S_{in}/3E_{ph} \qquad (3.41)$$

$$I = \frac{36000}{3 \times 346.48} = 34.6 \text{ A}$$

The cross-section area of the wire A_w:

$$A_w = \pi r_w^2 \qquad (3.42)$$

since,

$$I = A_w \cdot J_w \qquad (3.43)$$

$$A_w = \frac{I}{J_w} \qquad (3.44)$$

Substituting Eqn. 3.44 in 3.42:

$$\pi r_w^2 = I/J_w \qquad (3.45)$$

Equation 3.29 rewritten in order to calculate wire diameter:

$$D_W = 2\sqrt{\frac{I}{\pi \cdot J_w}} \qquad (3.46)$$

$$D_W = 2\sqrt{\frac{34.6}{\pi \cdot 5}} = 2.96 \text{ mm}$$

Using the value of the wire diameter, the wire type was selected as 10 AWG (American wire gauge) Table 3.1. AWG 9 was not selected since that particular type of wire is not found in the FEM model. Hence, the final corrected value of the wire diameter corresponding to AWG 10 is:

$$D_w = 2.6 \text{ mm}$$
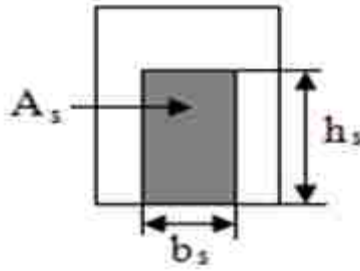
Figure 3.11 Slot model

❖ Height of the slot h_s:

$$h_s = A_s / b_s \qquad (3.47)$$

where A_s is the cross-section area of the slot.

If the slot is fully open the cross-section area of the slot is equal to cross-section area of the coil that is given by,

$$A_c = \frac{\pi (0.001 \cdot d_w/2)^2 \cdot N_c}{(K_{cu})} \qquad (3.48)$$

$$A_c = \frac{\pi (0.001 \cdot 2.6/2)^2 \cdot 82}{(0.5)} = 7.2560\text{e-}004 \qquad (3.49)$$

Since $A_s = A_c$ from Eqn. 3.47:

$$h_s = 47 \text{ mm}$$

All the above calculated parameters are enclosed in Table 3.2, carried out using m-file in Appendix-A and the schematic model with the dimensions is given in figure 3.13 and 3.14.

28

Table 3.1 American wire gauge[13]

AWG gauge	Conductor Diameter Inches	Conductor Diameter mm	Ohms per 1000 ft.	Ohms per km	Maximum amps for chassis wiring	Maximum amps for power transmission	Maximum frequency for 100% skin depth for solid conductor copper
OOOO	0.46	11.684	0.049	0.16072	380	302	125 Hz
OOO	0.4096	10.40384	0.0618	0.202704	328	239	160 Hz
OO	0.3648	9.26592	0.0779	0.255512	283	190	200 Hz
0	0.3249	8.25246	0.0983	0.322424	245	150	250 Hz
1	0.2893	7.34822	0.1239	0.406392	211	119	325 Hz
2	0.2576	6.54304	0.1563	0.512664	181	94	410 Hz
3	0.2294	5.82676	0.197	0.64616	158	75	500 Hz
4	0.2043	5.18922	0.2485	0.81508	135	60	650 Hz
5	0.1819	4.62026	0.3133	1.027624	118	47	810 Hz
6	0.162	4.1148	0.3951	1.295928	101	37	1100 Hz
7	0.1443	3.66522	0.4982	1.634096	89	30	1300 Hz
8	0.1285	3.2639	0.6282	2.060496	73	24	1650 Hz
9	0.1144	2.90576	0.7921	2.598088	64	19	2050 Hz
10	0.1019	2.58826	0.9989	3.276392	55	15	2600 Hz
11	0.0907	2.30378	1.26	4.1328	47	12	3200 Hz
12	0.0808	2.05232	1.588	5.20864	41	9.3	4150 Hz
13	0.072	1.8288	2.003	6.56984	35	7.4	5300 Hz

Table 3.2 Stator and rotor parameters

Stator core:	
- length **L**	432 mm
- width **W₁**	200 mm
- stator yoke **Y_s**	16 mm
- slot opening **b_s**	16 mm
- tooth width **b_t**	8 mm
- tooth hight **h_t**	48 mm
- pole pitch **τ_p**	72 mm
- permissible flux stator yoke B_y^s	1.8 T
- laminated Steel core	US steel type 2-S (B-H curve see fig. 3.12)
Rotor Core:	
- magnet Length **τ**$_m$	64.8 mm
- rotor yoke **Y_R**	24 mm
- permissible flux rotor yoke B_y^r	1.2 T
Winding:	
- number of phases **m**	3
- no. of poles **p**	6
- number of slots/phase/pole **q**	1
- turn number/coil **N_w**	82
- floater amplitude velocity **v_rm**	2.2 m/s
- permissible flux density in air-gap **B_av**	0.8 T
- air gap **g**	2 mm
- slot filling factor **K_cu**	0.6
Permanent Magnet:	
- magnet thickness **h_m**	9 mm
- residual magnetic flux density **B_r**	1.2 T
- coercive magnetic field intensity **H_c**	905000 A/m
- magnetic permeability **μ_m**	1.2×10^{-6} Hm^{-1}
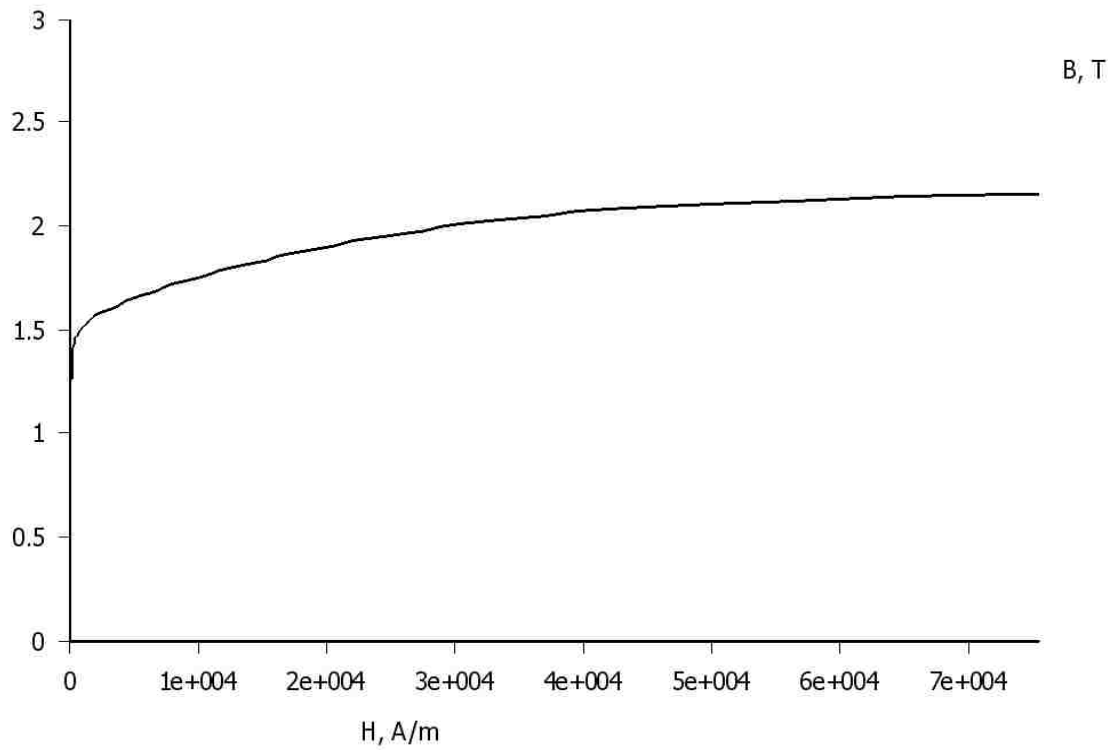
Figure 3.12 US steel type 2 – S B-H curve
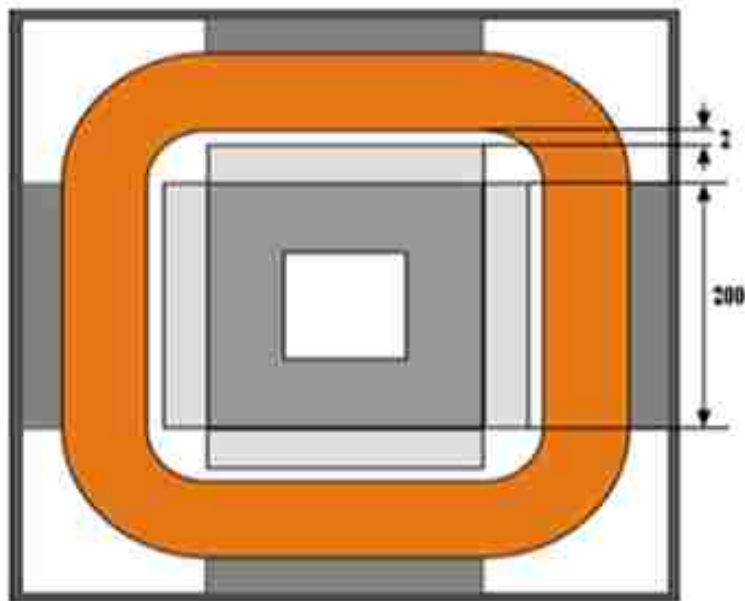
Figure 3.13 Structure of PM generator with dimensions top view
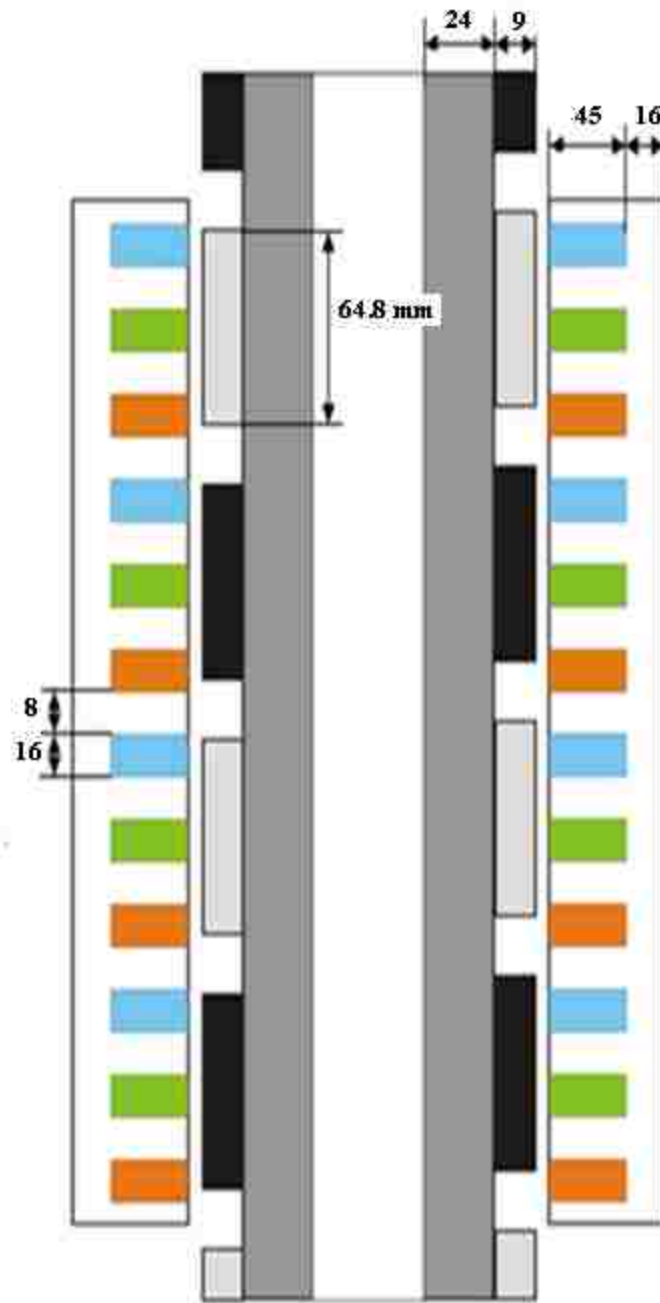
Figure 3.14 Structure of PM generator with dimensions cross-section view

CHAPTER 4

DETERMINATION OF GENERATOR ELECTRO-MECHANICAL PARAMETERS

In chapter 3 the main dimensions of the generator were determined as well as its winding. The method that was used is based on magnetic circuit model that has been defined by simplifying assumptions. To verify the obtained results the more accurate magnetic field model of the generator is applied and FEM is used to solve the differential field equations. It is also used to optimize the primary core and secondary parts of magnetic circuit of the generator and to determine the generator inductances.

4.1 Optimization of Stator and Rotor Yoke with FEM Model

The linear generator consists of four identical parts joined by the common winding. Thus only one part of the generator is considered (Figure 4.1). Since a single part of the generator does not change in shape and in width, it can be used in modeling the generator in 2-D space using FEMM 4.0 software.

The FEM model of a single part of the generator is shown in figure 4.2. The parameters of the materials assigned in this model are as follows:

➢ *Permanent Magnets*

   In the above model the secondary part consists of permanent magnets attached to the ferromagnetic plate. These permanent magents are made up of Neodymium Iron Boron (NdFeB).
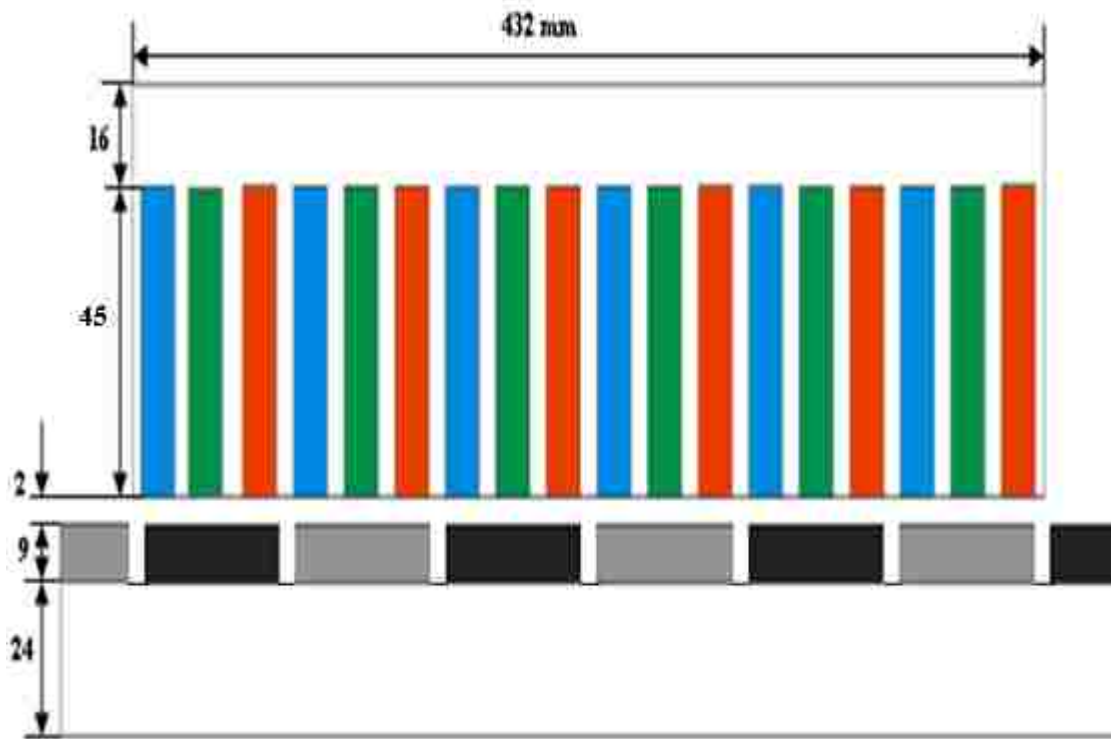
Figure 4.1 Main dimension of generator before optimization
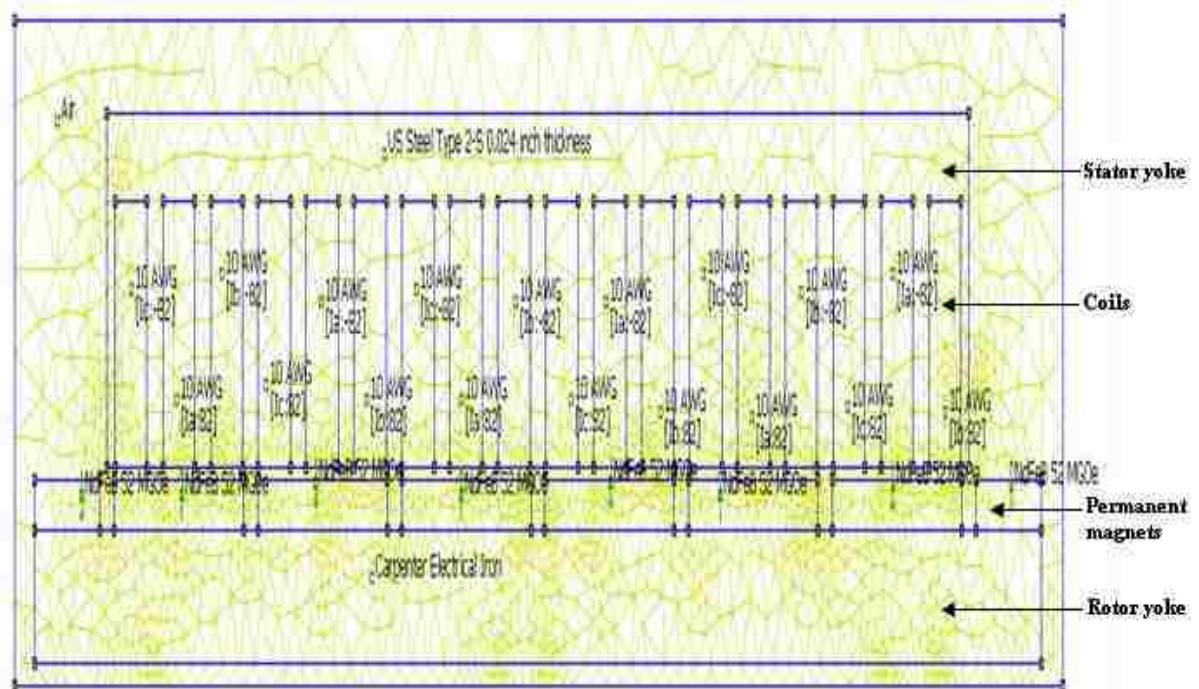
Figure 4.2 Linear 2D model of generator in FEMM 4.0

34

It has the following parameters assigned by the software:

B_r = 1.2 T Residual magnetic flux density.

H_c = 905000 A/m Coercive magnetic field intensity

μ = 1.2 x $^{10-6}$ magnetic permeability

➢ *Primary core part*

The laminated steel of US steel is used in the generator model and its magnetizing characteristic is as shown in the figure 4.3.
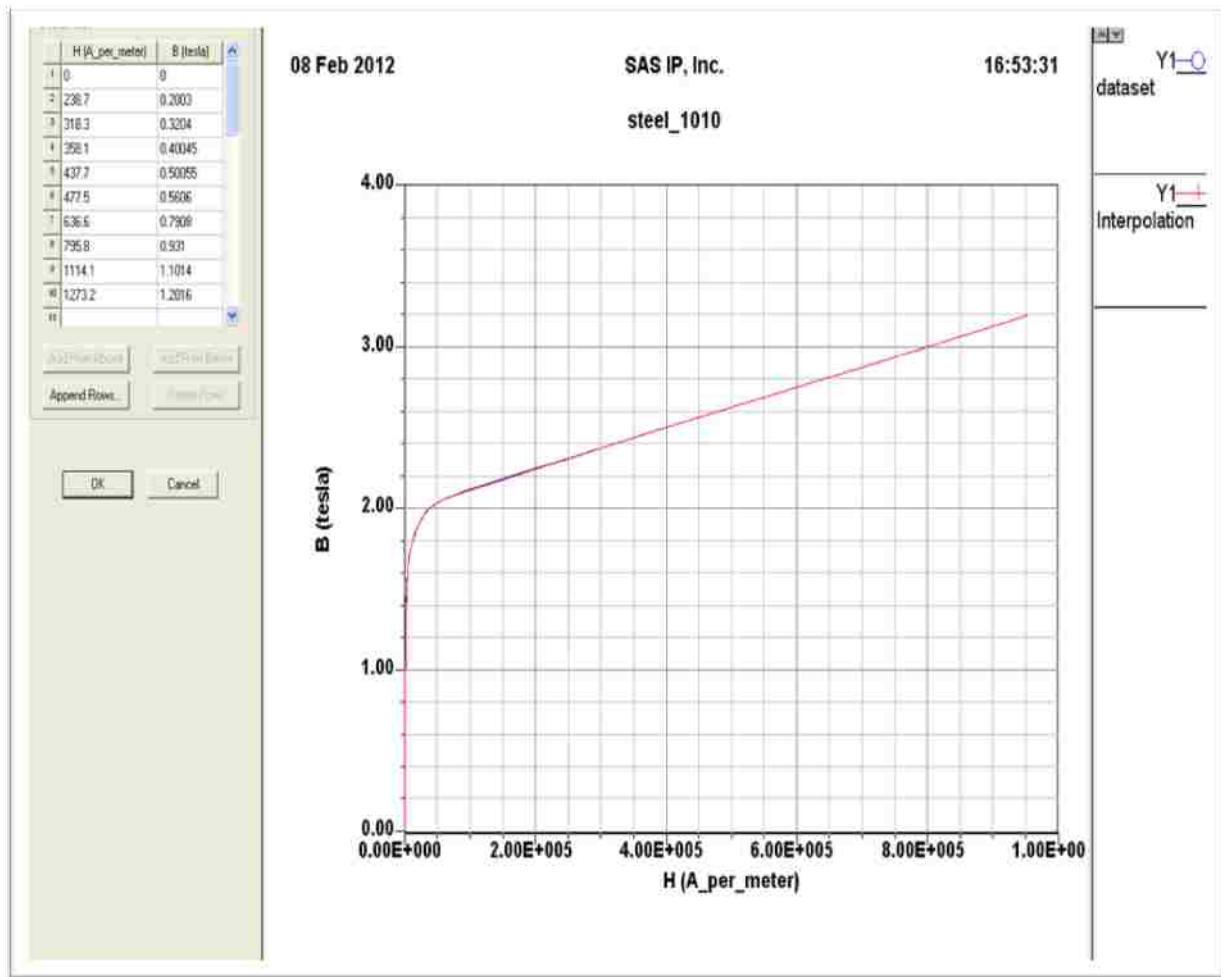
Figure 4.3 Magnetization characteristic of primary core

35

> *Secondary part core*

The solid iron is used in the generator model and its magnetizing characteristic is shown in figure 4.4.
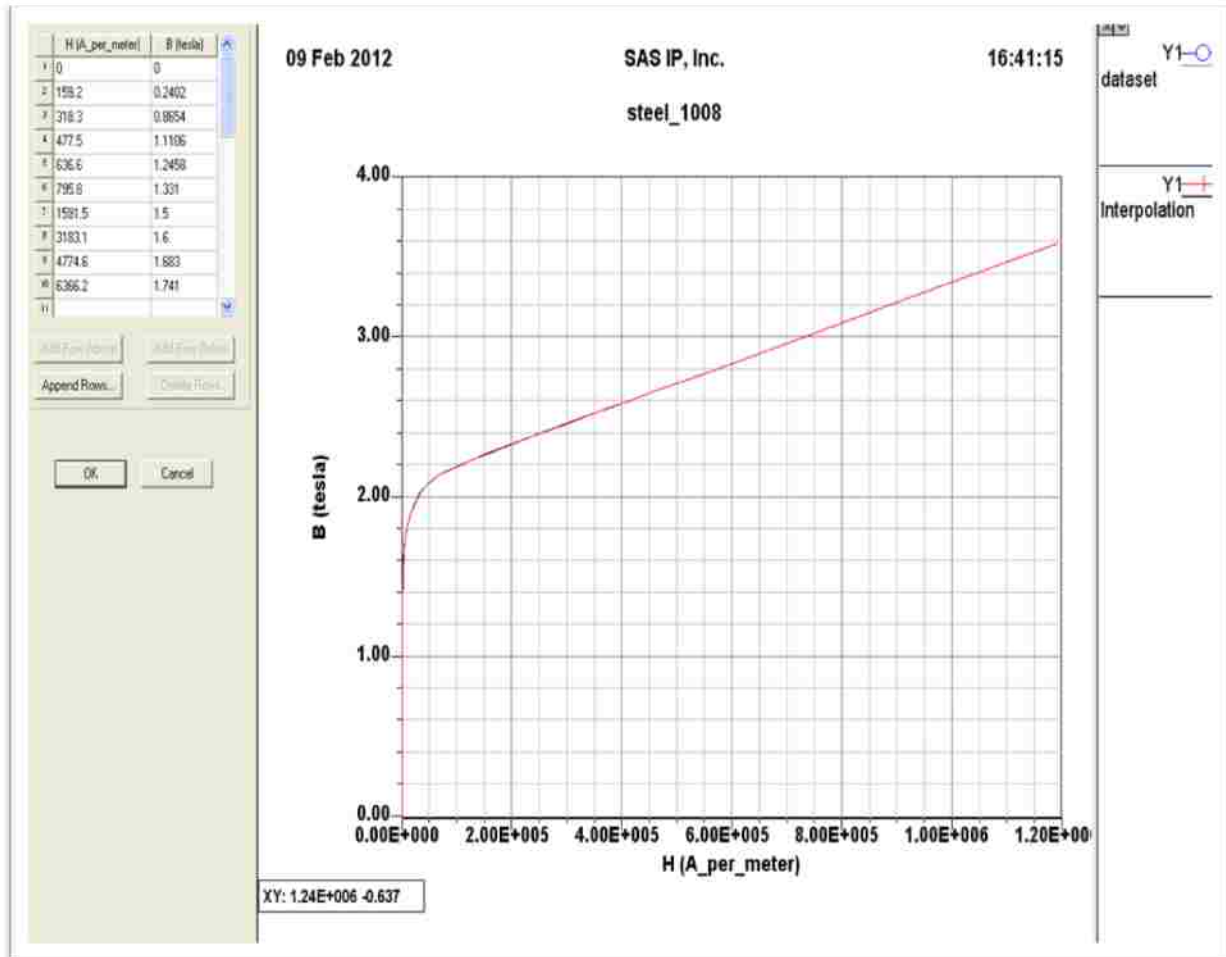
Figure 4.4 Magnetization characteristic of secondary core

To determine the flux density in the generator core and to optimize the core dimensions with respect to permissible flux density the FEM simulation was done at rated armature current. From Eqn. 3.22 its value is I = 34.6 A and its corresponding maximum value is 48.93 A. For time instance t = 0 the phase

currents are as follows (see phasor diagram in figure 4.5)

$$I_A(t=0)= 48.93A$$

$$I_B(t=0)= -24.46A$$

$$I_C(t=0)= -24.46A$$
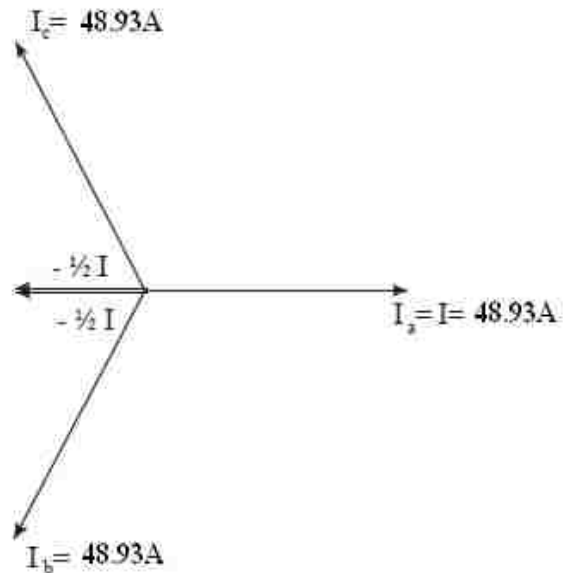
Figure 4.5 Phasor diagram of supply current at t=0

To avoid the excessive saturation of primary and secondary cores their permissible flux density has been assumed as B_y^s is 1.8 T and rotor yoke B_y^r is 1.2 T respectively.

The flux density distribution obtained for model with original dimensions of the generators primary and the secondary cores is shown in the figure 4.6.

(a)
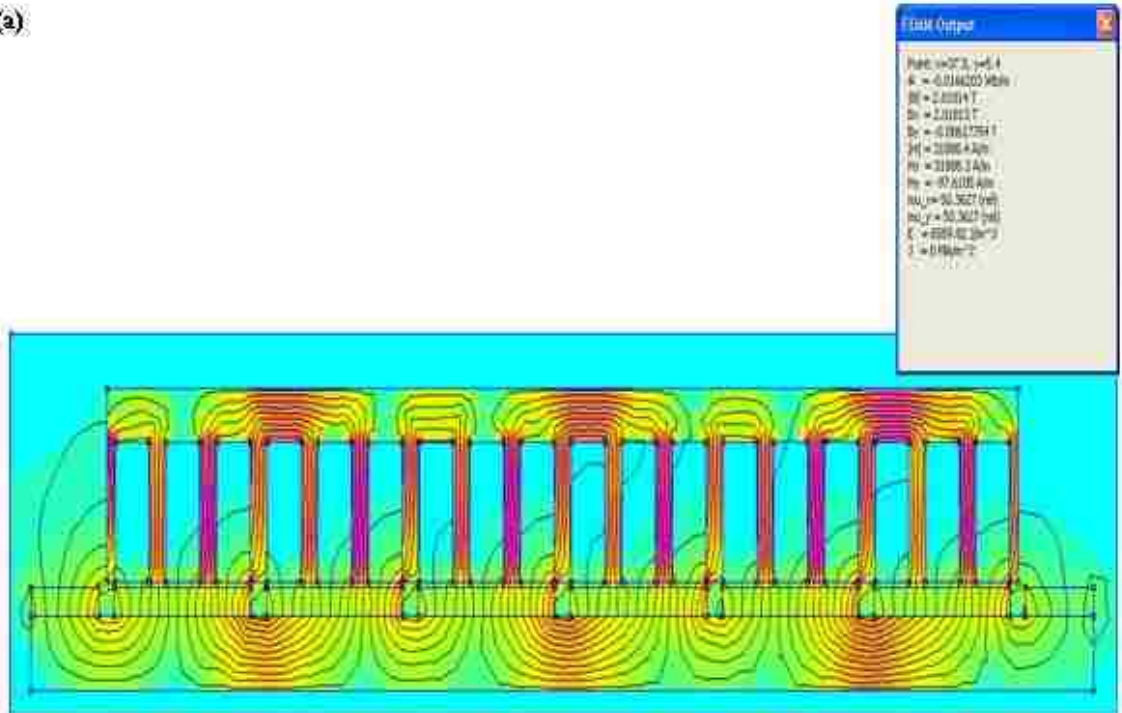
(b)
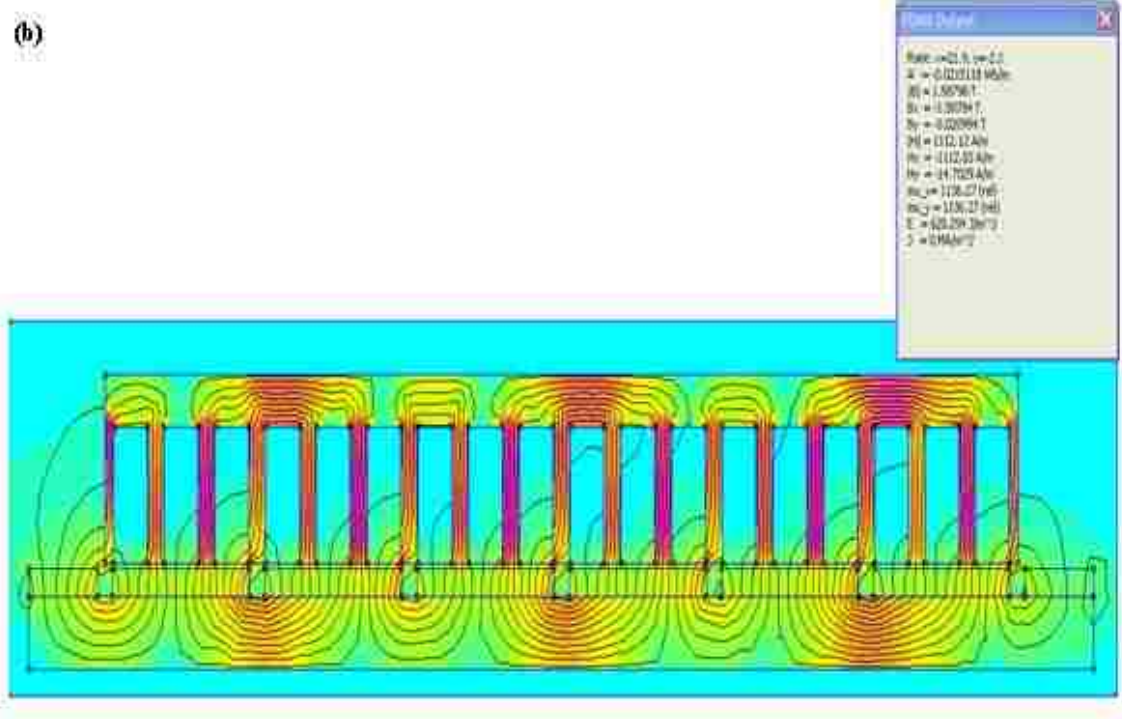
Figure 4.6 Flux density distribution before optimization (a) Primary core (b)
Secondary core

The maximum flux density in the primary core B_y^s is 2 T and in the

secondary core B_y^r is 1.5 T. The flux density value in the secondary and the

primary parts is too high with respect to the assumed permissible values (see

table 3.1).

To lower the flux density, the widths of the secondary and primary parts

have been increased to the values as shown in Table 4.1.

Table 4.1 Stator and rotor yoke parameters

	Before Optimization	After Optimization
Rotor yoke (mm)	24 mm	28 mm
Stator yoke (mm)	16 mm	20 mm
Flux in the rotor yoke B_y^r	>1.2 T	<1.2 T
Flux in the stator yoke B_y^s	>1.8 T	<1.8 T

The flux density distribution in the generator model with the modified

dimensions is shown in Figures 4.7 and 4.8.
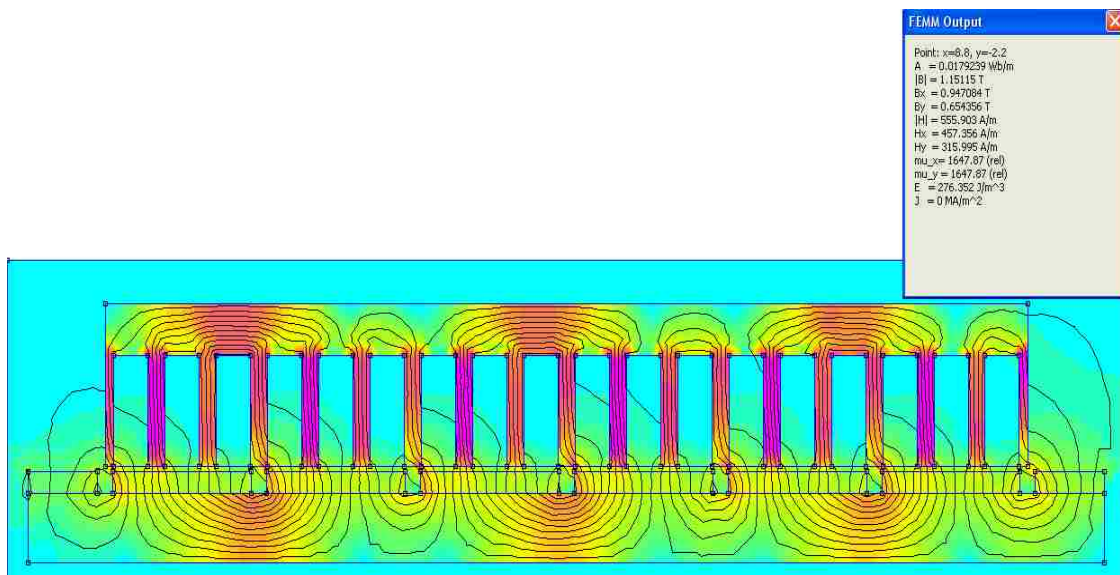
Figure 4.7 Flux density distribution in secondary after optimization
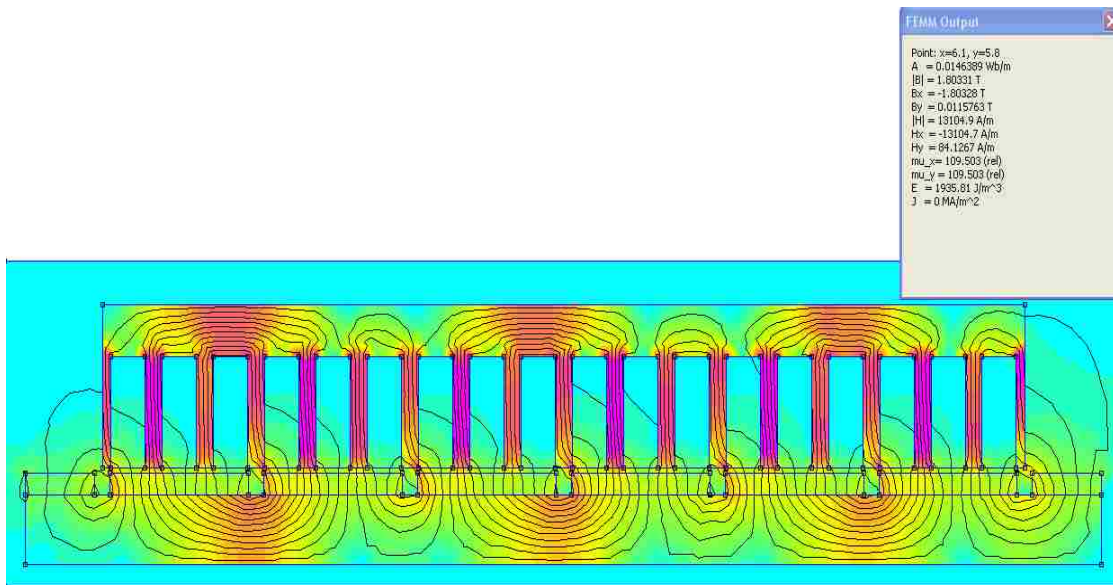
Figure 4.8 Flux density distribution in primary after optimization

As it is illustrated in the figure 4.9 the maximum flux density in the teeth

of the primary core is high and equal to 2.1 T. This is however acceptable.
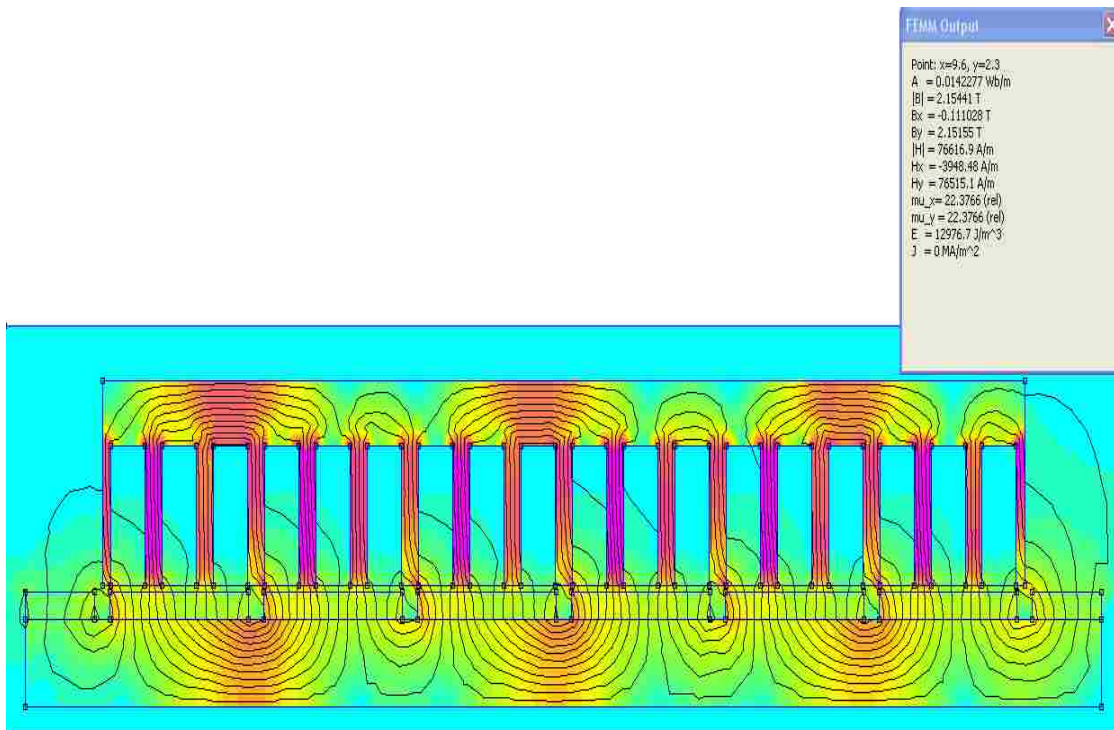
Figure 4.9 Flux density distribution in the teeth

4.2 3-D FEM model

    In order to validate the results obtained for 2-D model, the generator was modeled in 3-D space using the Maxwell 12v software package. The generator model is shown in figure 4.10 and 4.11.
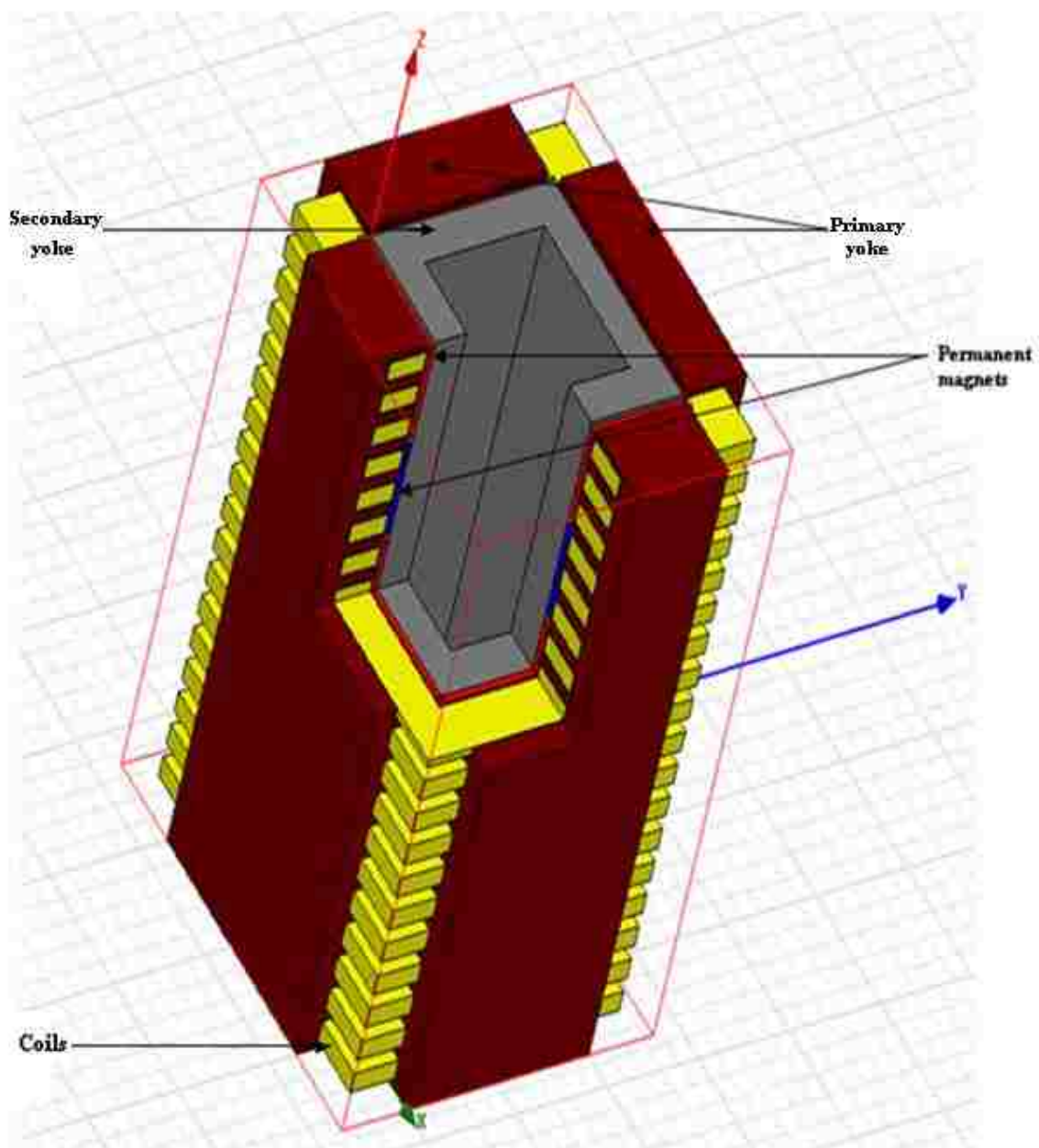
Figure 4.10 Model of generator in 3-D FEM
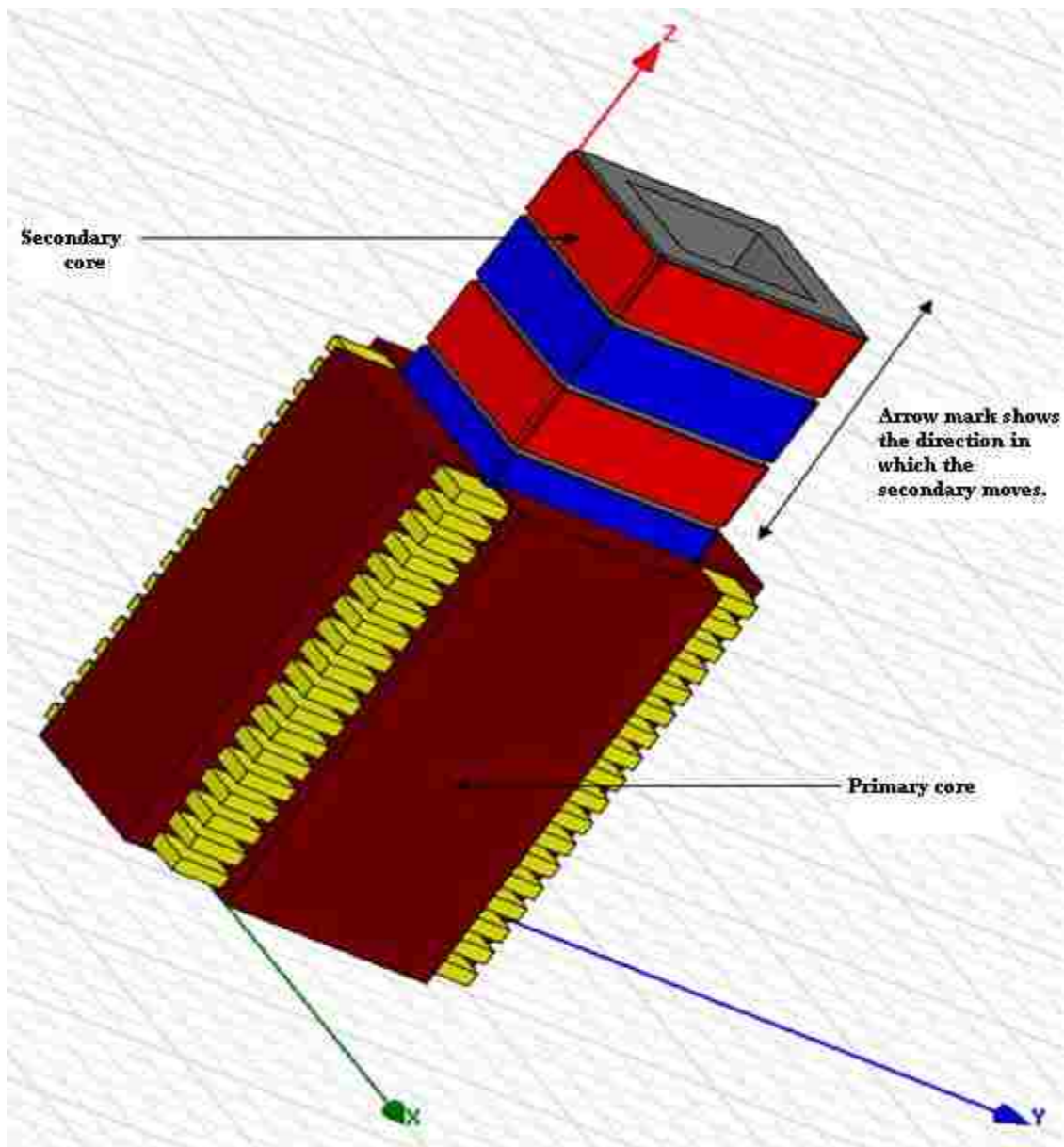
Figure 4.11 Schematic representation of secondary motion

The maximum flux density obtained from the 3-D model in primary and the secondary core is approximately 1.8 T and 1.2 T respectively as shown in figure 4.12.
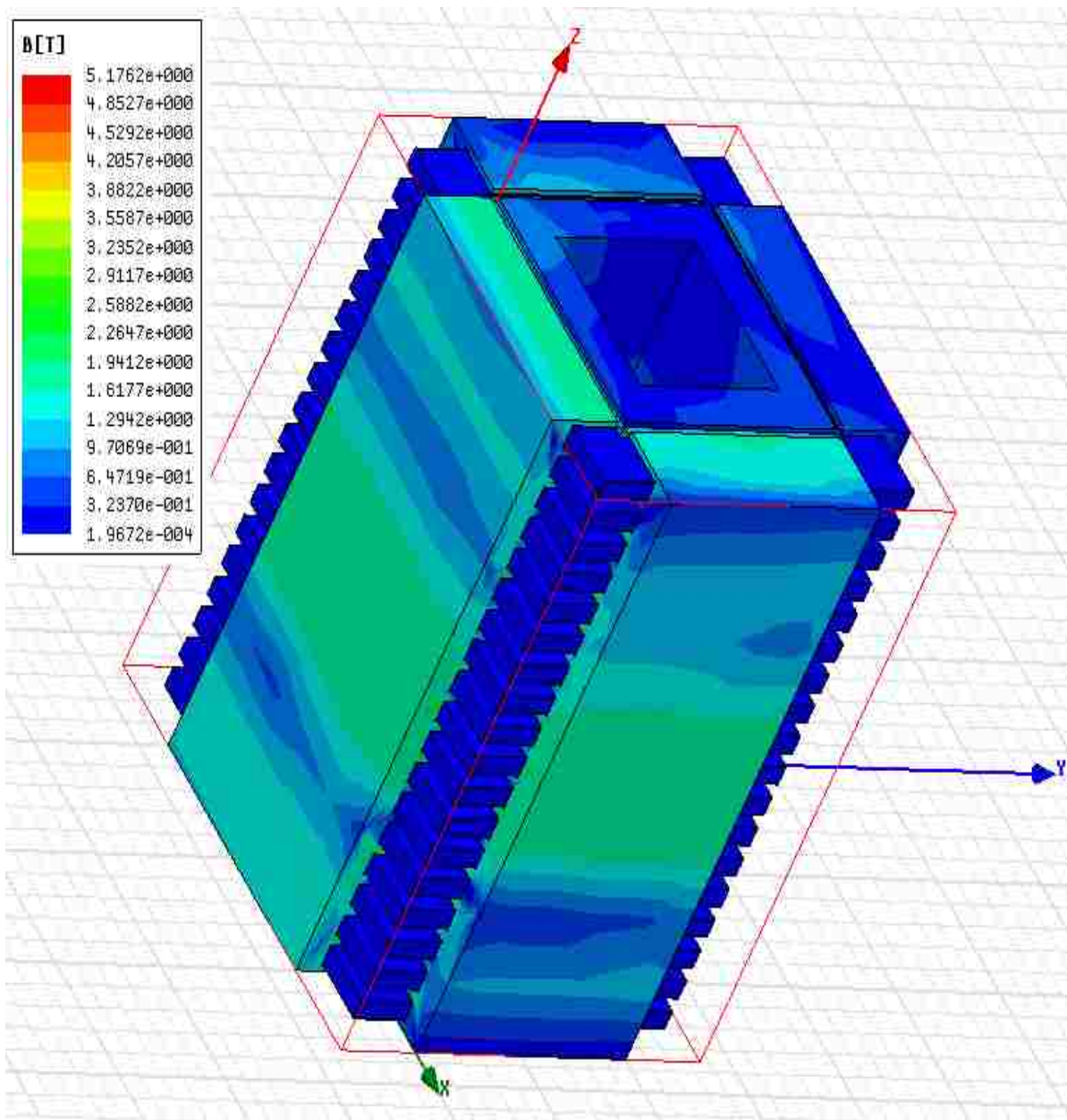
Figure 4.12 Flux density distribution in 3-D generator model

4.3 Winding Parameters

➢ *Phase resistance*

Due to modification of primary and secondary core the resistance of the winding has to be found for new winding length. The average length of the coil L_c can be found using the following equation (see figure 4.13):
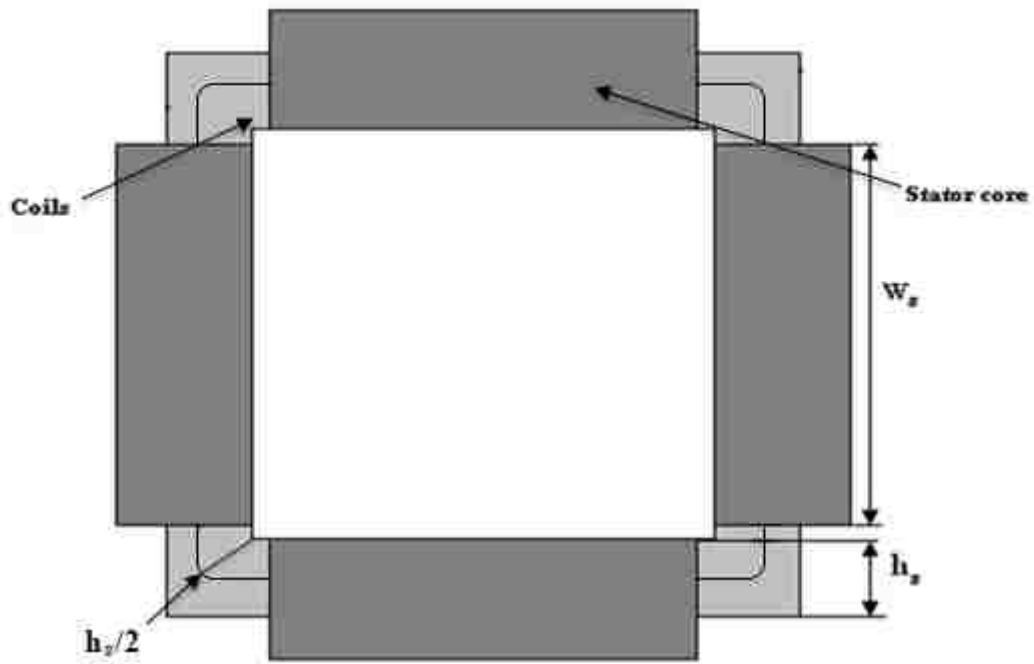
Figure 4.13 Scheme of coil for the calculation of the average length

From figure 4.13,

$$L_C = 2\pi \frac{h_s}{2} + M_S W_S \qquad (4.1)$$

$$L_C = 2\pi \frac{42}{2} + 4 \cdot 200 = 932 \text{ mm}$$

where, L_C - Average length of the coil

H_S - Height of the slot

W_S - Stator width

N_{Ph} - Number of turns per phase

R_{wpkm} - resistance per one kilometer for AWG wire [13]

The phase resistance R_{Ph} for the actual data of the winding is:

$$R_{ph} = R_{wpkm} \; 0.001 \; L_c \cdot N_{ph} \qquad (4.2)$$

$$R_{ph} = 1.5 \; \Omega$$

4.4 Inductance Calculation [12]

➢ **Self-Inductance:**

Before finding the inductance for the given model the following things has to be done in FEM Maxwell modelling:

- The matrix should be assigned to the model in order to get the solution for inductance values. This can be done by right clicking on Parameters icon and then selecting matrix from it as shown in figure 4.14.
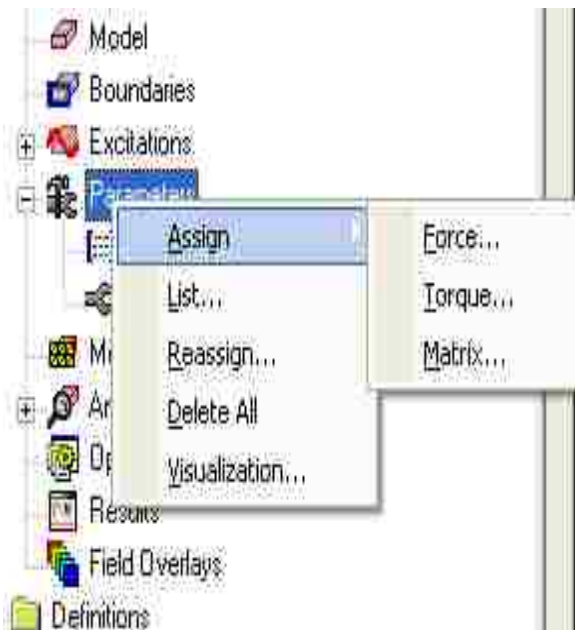
Figure 4.14 Selecting forms

- All the permanent magnets should be changed to air or vacuum.

- The model is assigned with rated current in phase 1 and zero current in the other two phases.

- The model is then simulated with 3 number of passes and with a error percent of 0.01%.

- Normally, the 3-D Maxwell software uses the following current and flux equation for solving inductance problem.

$$\begin{bmatrix} \lambda_1 \\ \lambda_2 \\ \lambda_3 \end{bmatrix} = \begin{bmatrix} L_{11} & L_{12} & L_{13} \\ L_{12} & L_{22} & L_{23} \\ L_{13} & L_{23} & L_{33} \end{bmatrix} \begin{bmatrix} i_1 \\ i_2 \\ i_3 \end{bmatrix}$$

- When only current i_1 is given the inductance matrix becomes like,

$$\begin{bmatrix} \lambda_1 \\ \lambda_2 \\ \lambda_3 \end{bmatrix} = \begin{bmatrix} L \end{bmatrix} \begin{bmatrix} 1 \\ 0 \\ 0 \end{bmatrix} = \begin{bmatrix} L_{11} \\ L_{12} \\ L_{13} \end{bmatrix}$$

- The value corresponding to L_{11} is the self-inductance value for loop 1. The L_{22} and L_{33} values are found in the similar ways. Then the average is taken:

$$L = (L_{11} + L_{22} + L_{33}) / 3 \qquad (4.3)$$

$$L = 0.096 \text{ H}$$

> **Mutual Inductance:**

- Similar steps are followed as in the case of the finding the self-inductance.

- The current in the phase 1 is supplied while the currents in the other two phases are zero.

46

- The magnets are turned to air or vacuum.

- The same matrix equation is used as discussed previously but instead of considering the diagonal values the off-diagonal elements like L_{12} and L_{13} are considered which corresponds to the mutual inductance of the generator. Then the average mutual inductance is calculated:

$$M = (L_{12} + L_{13} + L_{23}) / 3 \tag{4.4}$$

$$M = 0.019 \text{ H}$$

> **Synchronous Inductance**

Synchronous Inductance L_s of the stator is given by the formula,

$$L_s = \frac{\lambda}{i} \tag{4.5}$$

In the above equation 4.5, λ is the flux linkage generated by the current I in one phase plus the flux linkage contributed by the other two phases. Hence, the synchronous inductance can be expressed in the following equation,

$$L_s = L + M \tag{4.6}$$

$$L_s = 0.115 \text{ H}$$

Where,

L = Self-Inductance

M = Mutual Inductance

CHAPTER 5

ANALYSIS OF PERFORMANCE OF QUASI-FLAT PM LINEAR GENERATOR

The linear generator will operate under the variable speed, which depends on sea wave parameters such as length of the wave and its amplitude. In our analysis it is assumed that the speed changes sinusoidally. It means that the generator needs to be analyzed in dynamic conditions. However, the generator performance will be first determined at steady, mean secondary speed.

5.1 Performance of Generator at Constant Speed Operation

The analysis of generator performance under constant speed operation is done using generator equivalent circuit shown in Figure 5.1.
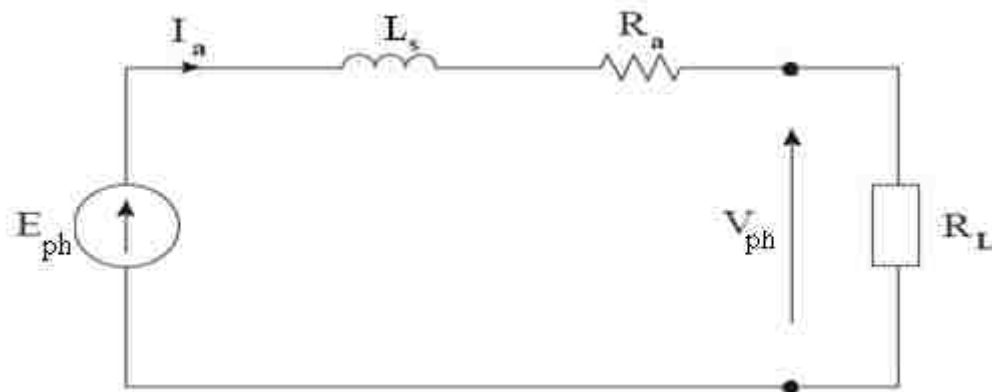
Figure 5.1 Equivalent circuit of generator for steady state operation

The power generated depends primarily on the load impedance if the speed is constant. It is assumed that the load impedance is pure resistive R_L. In this case the output power is:

$$P_{out} = 3\ R_L\ |I_a|^2 \tag{5.1}$$

The armature current I_a can be determined from voltage equation:

$$E_{ph} = V_a + I_a R_a + j\, 2\pi\, f\, L_a I_a \tag{5.2}$$

where: E_{ph} – Phase induced voltage

X_s – Synchronous reactance calculated as

$$X_s = 2\pi\, f\, L_a \tag{5.3}$$

f – Frequency calculated at average speed of the secondary part from the equation:

$$f = \frac{v_{av}}{2 \cdot \tau} \tag{5.4}$$

Thus the current is:

$$I_a = \frac{E_{ph}}{(R_L + R_a) + j\, 2\pi\, f\, L_a} \tag{5.5}$$

The emf E_{ph}, which is induced in the armature winding is given by:

$$E_{ph} = \frac{E_{ph\ m}}{\sqrt{2}} \tag{5.6}$$

where the amplitude of the voltage is

$$E_{ph\ m} = M_a \cdot W_a \cdot N_{ph} \cdot B_m \cdot u_{av} \tag{5.7}$$

where M_s – number of armature

W_s – Width of stator

N_{ph} – Number of turns per phase

B_m – flux density in the air-gap under the permanent magnet

obtained from FEM simulation

u_{av} – Average speed, which changes sinusoidally in time. Thus it is:

$$u_{av} = \frac{2}{\pi}\, u_m \tag{5.8}$$

where u_m is the speed amplitude.

Hence Eqn. 5.7 can be written as

49

$$E_{ph\ m} = K_E \cdot u \tag{5.9}$$

where the coefficient K_E is:

$$K_E = M_a \cdot W_a \cdot N_{ph} \cdot B_m \cdot u_{av} \tag{5.10}$$

The generator phase terminal voltage rms value is:

$$V_{ph} = I_a \cdot R_L \tag{5.11}$$

The input power at the average speed is calculated as:

$$P_{in} = 3\ \Re\ \{E_{ph} \cdot I_a^*\} \tag{5.12}$$

where I_a^* is the conjugate value of the phase current.

The generator efficiency calculated under assumption that the power losses in the primary core and mechanical losses are ignored and is expressed by the equation:

$$Eff = \frac{P_{out}}{P_{in}} \cdot 100\ \% \tag{5.13}$$

The calculation of generator performance has been done for constant speed and variable load resistance for the following data:

- E_{ph} – 346 V

- R_a – 1.5 Ω

- L_s – 0.115 H

The performance characteristics plotted as the functions of load resistance R_L are presented in Figure 5.2.
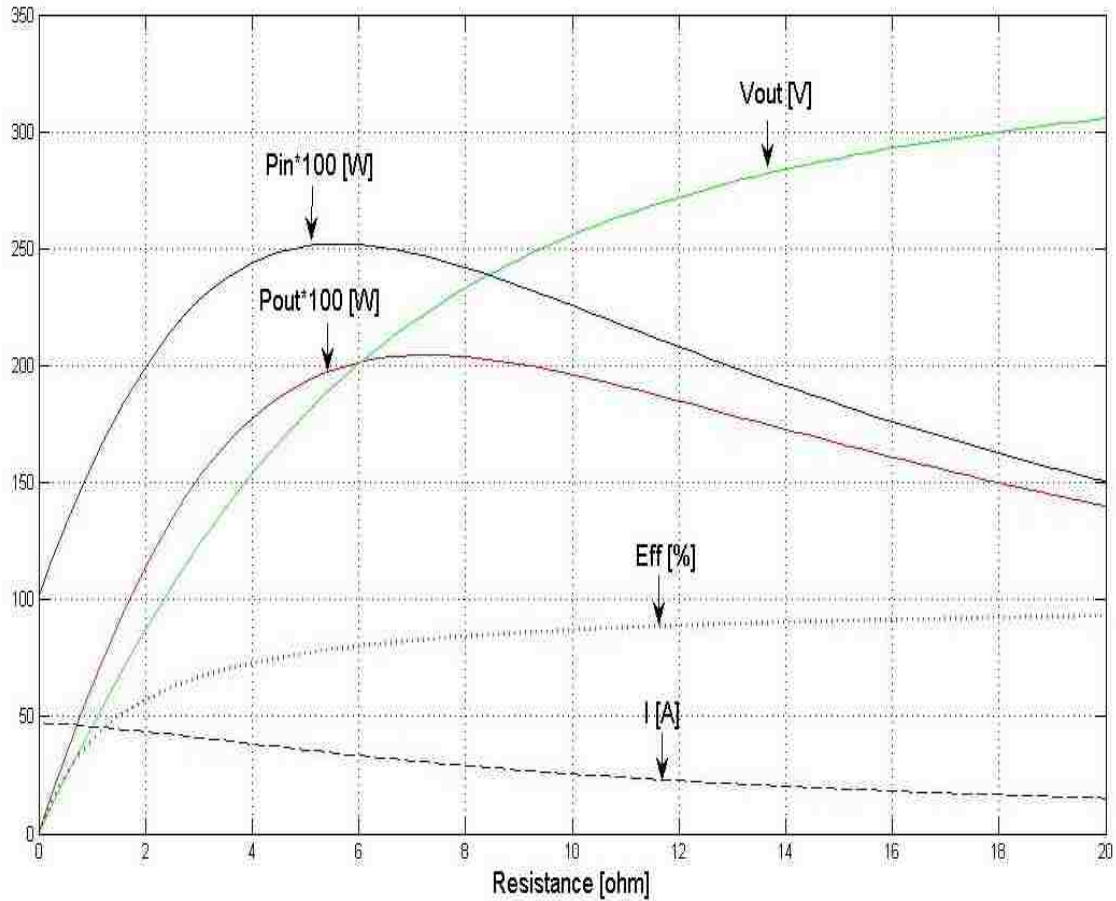
Figure 5.2 Performance characteristic as the functions of load resistance R_L

Varying load resistance R_L in the range 0 to 20 Ω the maximum output power at steady state is measured. The maximum output 21KW is obtained when the generator is loaded with a resistive load of 7.5Ω. At a resistive load, power is inversely proportion to the value of resistance (i.e. **P = V² / R**). Hence, increasing the resistance value, the current and power decreases which is evident from the graph shown. The maximum input power obtained is 25KW.

The values of the generator quantities obtained for the load resistance R_L = 7.5 Ω at maximum output power are enclosed in Table 5.1.

Table 5.1 Generator parameters at steady state speed

Generator Parameters	Values
Input Power P_{in}	25 KW
Output Power P_{out}	21 KW
Efficiency	85 %
Phase current I	34 A

The calculations were carried out using the program written in MATLAB shown as Pout.m file in Appendix-B.

5.2 Performance of generator in dynamic conditions

The dynamic model of the generator is defined by the following assumptions:

- The generator secondary part is driven by the sea wave with the sinusoidally changing speed,

- Due to surface mounted permanent magnets winding inductance is considered to be constant,

- The generator terminals are considered to be connected to the resistive load.

The generator equivalent circuit is shown in Figure 5.3. The generator is loaded by the load resistance R_L connected in wye. The voltage equation that describes this equivalent circuit is as follows:

52
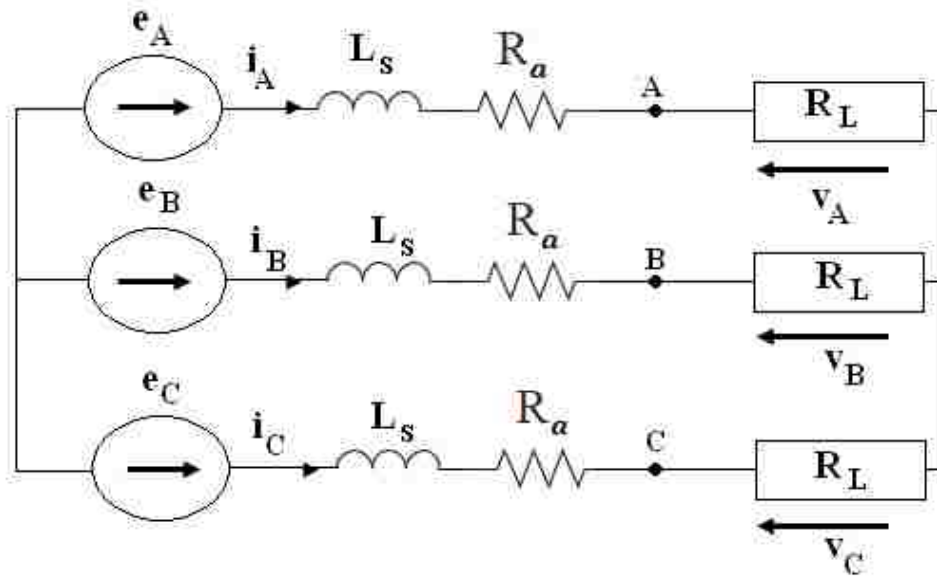
Figure 5.3 Equivalent Circuit of 3-phase winding of generator

$$e_A = R_a i_A + L_s \frac{di_A}{dt} + v_A \tag{5.14}$$

$$e_B = R_a i_B + L_s \frac{di_B}{dt} + v_B \tag{5.15}$$

$$e_C = R_a i_C + L_s \frac{di_C}{dt} + v_C \tag{5.16}$$

where, $e_{A,B,C}$ – phase induced voltages

R_a – phase resistance

L_a – phase inductance which is equal to the synchronous

inductance L_s

$v_{A,B,C}$ – generator terminal phase voltages

$i_{A,B,C}$ - phase currents

In general the voltage induced in the phase winding is given by:

$$e_{ph} = B(z) \cdot M_s \cdot W_s \cdot N_{ph} \cdot u(t) \tag{5.17}$$

where B(z) is the magnetic flux density in the air-gap that is assumed to change

sinusoidally along z axis according to equation:

53

$$B(z) = B_m \cos(\frac{\pi}{\tau}z) \qquad (5.18)$$

In Eqn. 5.18 B_m is the flux density in the air-gap under the permanent magnet obtained from the FEM simulation.

The Eqn. 5.17 can be written in the following form:

$$e_{ph} = K_E \cos\left(\frac{\pi}{\tau}z\right) u(t) \qquad (5.19)$$

where constant K_E:

$$K_E = M_a \cdot W_a \cdot N_{ph} \cdot B_m \qquad (5.20)$$

The speed u is changing sinusoidally according to equation:

$$u(t) = u_m \sin(\omega_m t) \qquad (5.21)$$

where u_m – speed amplitude

$\omega_m - 2\pi f_m$ is the angular frequency of the moving sea wave

Referring to 3-phase winding the induced emf are as follows:

$$e_A = k_E \cos\left(\frac{\pi}{\tau}z\right) u(t) \qquad (5.22)$$

$$e_B = k_E \cos\left(\frac{\pi}{\tau}z - \frac{2\pi}{3}\right) u(t) \qquad (5.23)$$

$$e_C = k_E \cos\left(\frac{\pi}{\tau}z - \frac{4\pi}{3}\right) u(t) \qquad (5.24)$$

To simulate the operation of the generator in dynamic conditions the block diagram was developed in MATLAB/SIMULINK which is shown in the Figure 5.4.

In this diagram the input quantity is the speed of the generator. The output quantities are:

➢ **Input power:**

$$P_{in} = e_A i_A + e_B i_B + e_C i_C \qquad (5.25)$$

54

➢ **Electromotive force:**

$$F_{em} = \frac{p_{in}}{u(t)}$$ (5.26)
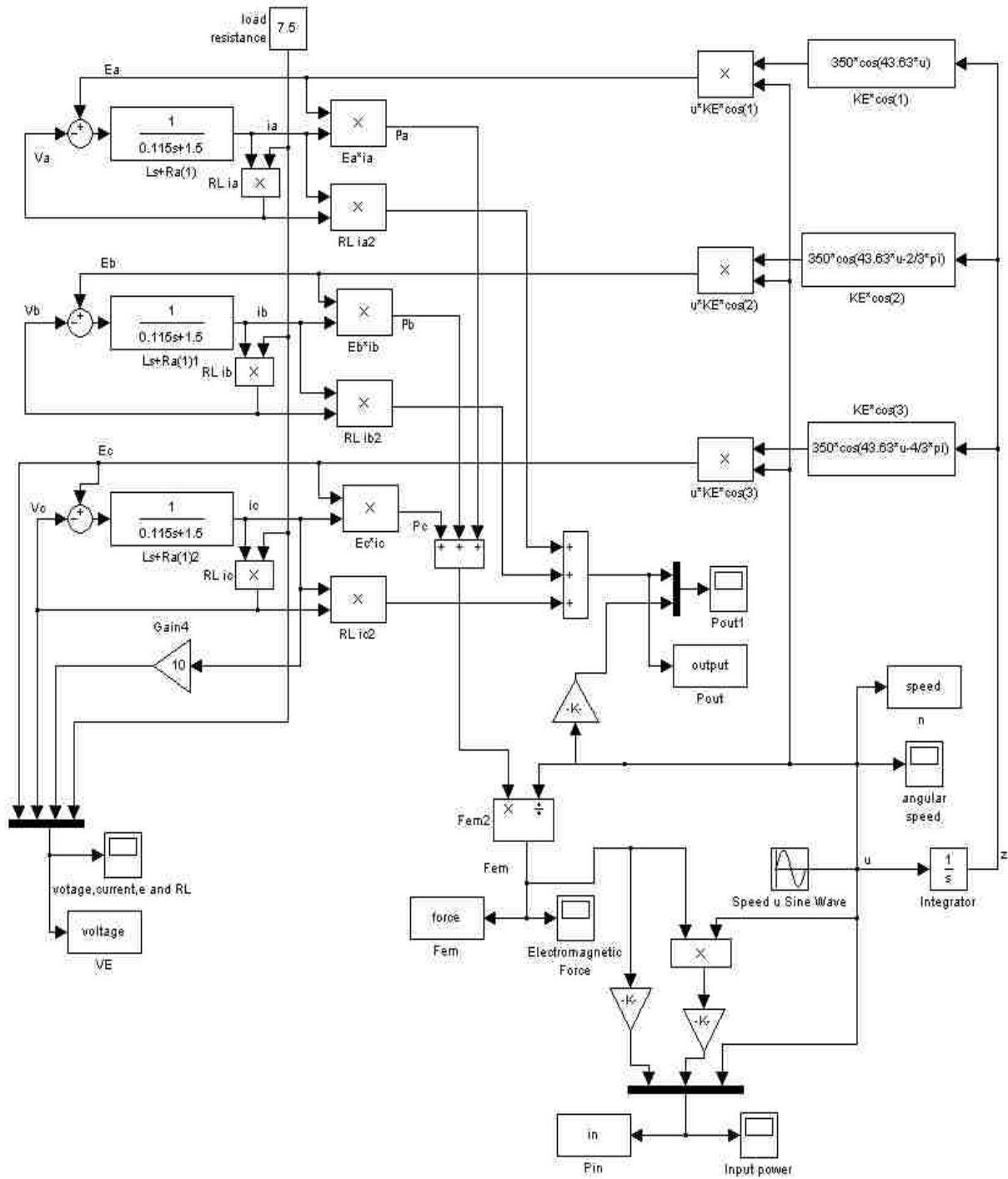
Figure 5.3 Simulink model of quasi flat linear PM generator

The simulation was carried out for the parameters enclosed in Table 5.2.

55

Table 5.2 Input parameters of SIMULINK file

PARAMETER	VALUE
Load Resistance R_L	7.5 Ω
Synchronous Inductance L_s	0.115 H
Armature resistance R_a	1.5 Ω
Secondary speed amplitude u_m	2.2 m/s
Voltage constant K_E	350 V.s/m
Pole pitch τ	0.072 m

The results of simulation are shown in Figures 5.4, 5.5 and 5.6. The waveforms were plotted using program written in MATLAB, which is shown as final.m file in Appendix-C.
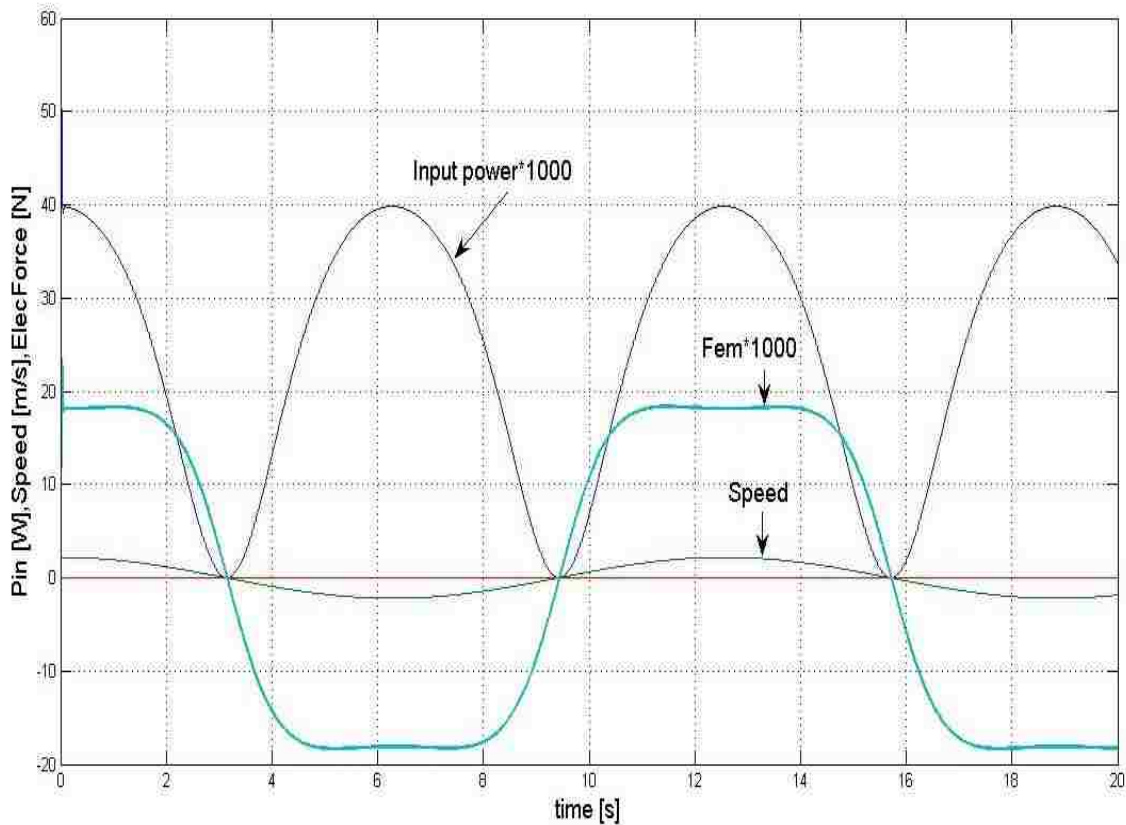
Figure 5.4 Dynamic characteristics of input power, Electromagnetic force and speed
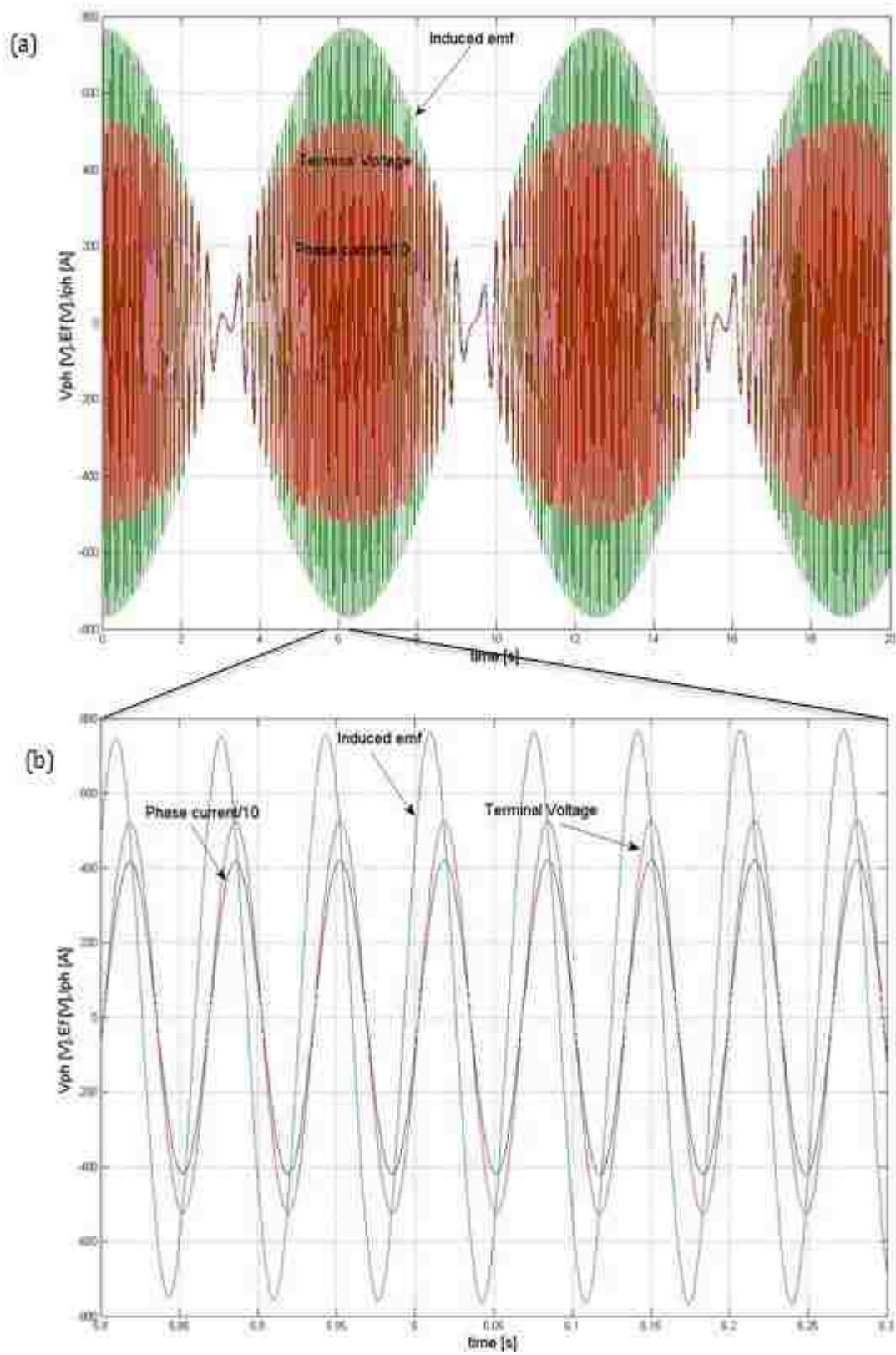
Figure 5.5 Terminal voltage, induced voltage and phase current vs (a) time interval (0-20) (b) time interval (5.8-6.3)
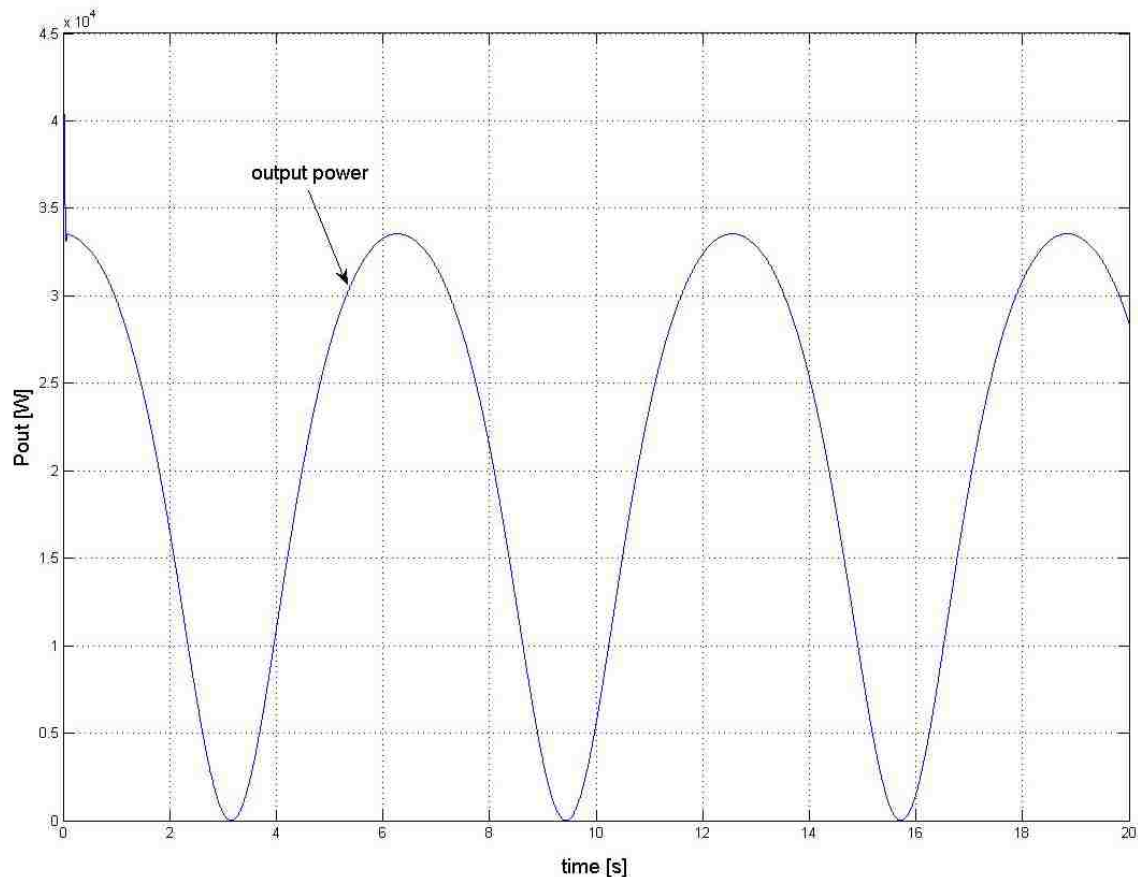
Figure 5.6 Output power characteristic at dynamic conditions

The generator is operated at sinsusoidal speed (see figure 5.4). Due to this all parameters like the terminal voltage, power and phase induced voltage show sinusoidal characteristics(see figures 5.4, 5.5 and 5.6). The maximun input and output power of the generator is 40KW and 34KW respectively. Its average power is 25KW and 21KW respectively, which is same as read from the steady state characteristic (see figure 5.2) with steady average speed. From figure 5.6 it is found that the terminal voltage and the phase current are in phase with each other since the generator is loaded with a pure resistive load. Initially the speed and power values are maximun. But as the speed decreases the power also decreases and when speed reaches zero all values are zero. The position of the secondary can be explained from the speed graph (see figure 5.4). Initially the

secondary is at its reference position or starting point where speed is at its maximum value. Now, when the secondary part moves upwards the speed decreases. When it reaches the upper limit, the value of speed is zero. Then, the moving part moves down with an increase in speed until it reaches the bottom limit.

CHAPTER 6

CONCLUSION

6.1 Conclusion

The performance of linear quasi-flat PM 3 phase generator driven by sea wave energy has been studied. The linear generator with quasi-flat linear machine structure was designed using the magnetic circuit. By applying FEM the magnetic circuit was optimized and parameters of equivalent circuit were determined.

The performance of generator operation were studied in steady-state and dynamic conditions using MATLAB/SIMULINK. From the analysis of the generator operation the following conclusions can be specified:

➢ As speed is changing sinusoidally (following the sea wave motion) the amplitude of electromotive force as well as of the terminal voltage and current also changes sinusoidally. This makes the output power as well as electromagnetic force changing sinusoidally too.

➢ The output and the input powers of the generator at rated speed of 2.2 m/s are 34KW and 40KW respectively.

➢ The maximun output power is generated when the generator is connected to a resistive load of 7.5Ω.

➢ The value of power and current decreases as the resistance increases since they are inversely proportional to the value of resistance

➢ The terminal voltage and the output current are in phase with each other due to pure resisitive load, while the induced electromotive force is leading with respect to terminal voltage.

➢ The efficiency obtained for rated average speed of 1.4 m/s and at rated load resistance (of 7.5Ω) is equal to 85%.

6.2 Future Scope of Study

The efficiency can be improved furthur by reducing the reactance which can be achieved by reducing the frequency at which the generator operates. Futhur, the proposed structure of generatot can be built and the results can be compared with that of the simulated results.

REFERENCES

[1]   Sabzehgar, R. and M. Moallem, *A review of ocean wave energy conversion systems.* Electrical Power & Energy Conference (EPEC), 2009 IEEE: p1-6.

[2]   Rodrigue, L., *Wave power conversion systems for eletrical energy production.*

[3]   Polinder, H., M.E.C. Damen, and F. Gardner, *Linear PM Generator system for wave energy conversion in the AWS.* Energy Conversion, IEEE Transactions on, Sept. 2004. **vol.19,** (no.3,): p. pp. 583- 589.

[4]   Wu, F., et al., *Modeling and Control of AWS-Based Wave Energy Conversion System Integrated Into Power Grid.* Power Systems, IEEE Transactions on, Aug. 2008. **23**(3): p. pp.1196-1204.

[5]   Sa da Costa, J., et al., Control Applications, 2003. CCA 2003. Proceedings of 2003 IEEE Conference on Modeling of an ocean waves power device AWS. **1**: p. 618-623.

[6]   Polinder, H., et al., *Conventional and TFPM linear generators for direct-drive wave energy conversion.* Energy Conversion, IEEE Transactions on. **20**: p. 260-267.

[7]   Vermaak, R.K., M.J., *Design of a novel air-cored permanent magnet linear generator for wave energy conversion.* Electrical Machines (ICEM), 2010 XIX International Conference on: p. pp.1-6.

[8]   Pirisi, A., G. Gruosso, and R.E. Zich, *Novel modeling design of three phase tubular permanent magnet linear generator for marine applications*, in *Power Engineering, Energy and Electrical Drives, 2009. POWERENG '09. International Conference on* March 2009. p. 78-83.

[9]   Delli Colli, V., R. Di Stefano, and M. Scarano, *A tubular generator for marine energy direct drive applications.* Electric Machines and Drives, 2005 IEEE International Conference on p. 1473-1478.

[10]   Li, Q.-f., J. Xiao, and Z. Huang, *Flat-type permanent magnet linear alternator: A suitable device for a free piston linear alternator.* Journal of Zhejiang University - Science A
Cover. **10**(3).

[11]   Prado, M. and H. Polinder, *Direct drive in wave energy conversion — AWS full scale prototype case study.* Power and Energy Society General Meeting, 2011 IEEE: p. 1-7.

[12]   Corporation, A., *Introduction to Scripting in Maxwell – Version 12.*

[13]   *Power stream: Wire gauge and current limits.*

APPENDIX-A: LINEAR_GENERATOR.M

```
% designing of PM 3-phase linear generator
%Data
clc;
m=3;            %number of phases
Sin=36000;      %input power
E=600;          %line induced voltage
Eph=E/sqrt(3);  %phase induced voltage
vrm=2.2;        %floater velocity amplitude
vav=2/pi*vrm;   %average velocity
p=6;            %number of magnetic poles
q=1;            %number of slots per phase per pole
Ms=4;           %number of armatures
Bav=0.8;        %average flux density in the air-gap
Cm=0.9;         %coefficient for air-gap flux density: Cm=Bav/Bm
Bm=Bav/Cm;      %air-gap flux density under magnets
Br=1.2; Hc=905000;%PM parameters
miuo=4*pi*10^(-7);  %magnetic permeability of vacuum
g=0.002;        %air-gap
Bys=1.8;        %flux density in the stator yoke
Byr=1.2;        %flux density in the rotor yoke
Js=120000;      %current loading (linear current density of the stator
Jw=5;           %wire current density
Kcu=0.6;        %winding filling factor



%calculation of the stator and rotor core dimensions
WsLs=Sin*sqrt(2)/(Ms*Bm*Js*vav); %stator surface
Ws=input('stator width=')
Ls=WsLs/Ws;     %stator length
tau=Ls/p;       %pole-pitch
%tau=input('pole pith after dimension change')
f=vav/(2*tau);  %frequency
taut=tau/(m*q); %tooth pitch
bs=2/3*taut     %slot width
bs=input('slot width=')
taut=3/2*bs;    %corrected tooth pitch
tau=m*q*taut;   %corrected pole pitch
Ls=p*tau;       %corrected stator length
bt=1/3*taut;    %tooth width
Kc=taut*(5*g+bs)/(taut*(5*g+bs)-bs^2); %Carter's coefficient
geq=Kc*g;       %equivalent air-gap
hM=geq*Br*Bav/(miuo*Hc*(Br-Bm))  %permanent magnet thickness for
Neodymium
%magnets with straight line characteristic
hM=input('permanent magnet thickness='), %chosen permanent magnet thickness
Ys=Bav/Bys*tau/2; %stator yoke thickness
```

63

```matlab
Yr=Bav/Byr*tau/2; %rotor yoke thickness
tauM=Cm*tau;      %PM length

%calculation of the winding parameters
Nph=Eph*sqrt(2)/(Ms*Ws*Bm*vav)  %number of turns per phase
Nc=Nph/(q*p)         %number of turns per coil
Nc=input('The number of turns per coil Nc=')
Nph=Nc*(q*p)         %number of turns per phase
Eph=Ms*Ws*Nph*Bm*vav/sqrt(2) %phase emf for given turn number
E=sqrt(3)*Eph    %line induced voltage
I=Sin/3/Eph        %phase current
Dw=2*sqrt(I/pi/Jw) %wire diameter
Dw=input('wire diameter Dw=')
Rwpkm=input('resistance per 1km Rw/km=')
Jw=I/(pi*(Dw/2)^2);  %actual current density
Ac=pi*(0.001*Dw/2)^2*Nph/(q*p*Kcu)  %coil cros-section area
hs=Ac/bs          %hight of the slot
hs=input('chosen hight of slot=')
Lc=2*pi*hs/2+Ms*Ws;   %average length of the coil
Rph=Rwpkm*0.001*Lc*Nph; %coil resistance
Sin=3*Eph*I;         %actual input power
VRph=Rph*I;           %resistance voltage drop
Vph=Eph-VRph;         %phase voltage
V=sqrt(3)*Vph;      %line voltage
Sout=3*Vph*I;        %output power

%summary of the motor parameters
%stator dimensions
Ws_Ls_p_tau_bs_hs_bt_Ys=[Ws Ls p tau bs hs bt Ys]

%Rotor dimensions
Yr_hM_taum_Wm_g=[Yr hM tauM Ws g]

%Winding parameters
Nc_Dw_Kcu_Jw_Rph=[Nc Dw Kcu Jw Rph]

%Electromechanical parameters
Sout_Sin_V_Vph_I_E_Eph_vav_f=[Sout*0.001 Sin*.001 V Vph I E Eph vav f]
```

APPENDIX-B: POUT.M

```
Rl=0:20/100:20;
f=9.86;
Eph=346;
Ra=1.5;
Xs=0.115*9.86*2*pi/1;
Ia=Eph./(Ra+Rl+j*Xs);
I=abs(Ia);
Pou=3*I.^2.*Rl;
Pin=3*real(Eph.*conj(Ia));
Eff=Pou./Pin*100;
Vou=Rl.*I;

CLF,
figure(1),
plot(Rl,Pou/100,'r',Rl,Vou,'g',Rl,I,'--',Rl,Pin/100,'b',Rl,Eff,':'),xlabel('Resistance [ohm]'),grid,
gtext('Pout*100     [W]'),gtext('Vout     [V]'),gtext('I     [A]'),gtext('Pin*100 [W]'),gtext('Eff [%]'),
```

APPENDIX-C: FINAL_GRAPH.M

```
load force Fem; load speed n; load voltage VE; load output Pout; load in Pin
t=Fem(1,:);n=n(2,:);Ia=VE(4,:);Vph=VE(3,:);Ef=VE(2,:);Pout=Pout(2,:);Pin=Pin
(3,:);

CLF
figure (1)
plot(t,Pin,t,n,t,Fem/1000),xlabel('time [s]'),
ylabel('Pin [W],Speed [m/s],ElecForce [N]'),grid,
gtext('Input power*1000'),gtext('Speed'),gtext('Fem*1000'),

figure (2)
plot(t, Vph,t,Ef,t,Ia),xlabel('time [s]'),
ylabel('Vph [V],Ef [V],Iph [A] '),grid,
gtext('Terminal Voltage'),gtext('Induced emf'),gtext('Phase current * 10'),

figure (3)
plot(t,Pout),xlabel('time [s]'),
ylabel('Pout [W]'),grid,
gtext('output power'),
```

VITA

Rajkumar Parthasarathy was born in 1986 in Chennai, Tamil Nadu, India. He finished his Bachelor of Engineering in Electrical and Electronics Engineering from Anna University on May 2008. After which he worked in Orchid Chemicals and Pharmaceuticals Ltd. as Engineering Trainee. In August 2009 he came to Louisiana State University to pursue his master's in electrical engineering. He is currently a candidate for the degree of Master of Science in Electrical Engineering, which will be awarded in May 2012.